

Chapter 2 Geochemical survey

2-1 Objective

The objective of the geochemical survey is to identify targets likely to represent potentially significant mineralization.

2-2 Method

2-2-1 Sampling

Almost all samples were collected from outcrop, in total 409 locations in the survey area. In the case of talus fines, the minus 80 mesh fraction was collected.

2-2-2 Chemical analysis

All samples were analyzed for the 8 elements, Au, Ag, As, Sb, Cu, Mo, Pb, and Zn, known to be enriched in porphyry copper type systems. Analysis were carried out by CHEMEX Ltd, Vancouver Canada. The lower detection limits for each element are as follows; Au: 5 ppb, Ag, Sb: 0.2 ppm, As, Cu, Mo, Pb, Zn: 1 ppm.

2-3 Results

The geochemical analyses for all samples are shown in Appendix 4. The basic statistical values of the elements are shown in Table 2-2-1. Analytical values were converted into natural logarithms. Half the value of the lower limit has been used for conversion of statistical processing. The correlation coefficients are shown in Table 2-2-2. Plots were constructed of cumulative frequency vs. log concentration (Appendix 5).

2-3-1 Determination of threshold values

Threshold values were chosen corresponding to the value of the inflection point between the overlapping background and anomalous populations. These threshold values are listed in Appendix 5.

2-3-2 Distribution of geochemical anomalies

The distribution of geochemical anomalies are shown in Fig. 2-2-1 and summarized below.

Au

The background value for Au is 3 ppb. Only 10% of all 409 samples are anomalous. Anomalies are located in the Rinconada Prospect, the southern ridge of Rinconada and

Table 2-2-1 Basic statistical values of elements analysed

	Au	Ag	As	Cu	Mo	Pb	Sb	Zn
Sum	3002.5	298.8	3232	114391	1082	52834	417.4	42073
Maximum	430	65	130	22700	385	10000	60	5200
Minimum	2.5	<0.2	<1	<1	<1	<1	<0.2	<1
Average	7.34	0.73	7.90	279.68	2.65	129.18	1.02	102.87
Standard deviation	33.49	4.30	11.57	1427.38	20.32	872.15	3.48	309.82

Table 2-2-2 Correlation coefficients among each element analysed.

Au	1.00																			
Ag	0.35	1.00																		
As	0.08	0.04	1.00																	
Cu	0.26	0.44	0.12	1.00																
Mo	0.10	0.16	0.04	0.23	1.00															
Pb	0.18	0.55	-0.11	0.19	-0.01	1.00														
Sb	0.25	0.40	0.27	0.21	-0.05	0.47	1.00													
Zn	0.12	0.37	-0.07	0.35	-0.08	0.25	0.40	1.00												
	Au	Ag	As	Cu	Mo	Pb	Sb	Zn												

around Quebrada Emiqueta. Weak anomalies are distributed in the Central Prospect and at the La Escondida mine. No anomalies are apparent in the La Guanaca Prospect. The distribution of Au anomalies corresponds to higher concentration of Au in the quartz vein in the Rinconada Prospect than the other prospects (Table 2-3-1, Fig 2-3-3).

Ag

The background value for Ag is 0.56 ppm. Only 10% of all 409 samples are anomalous. Silver has a more limited distribution than gold. The anomalies are distributed in the Rinconada, La Guanaca, Central, and La Escondida Prospects, however are relatively low with a maximum concentration of only 65 ppm.

As

The background value for As is 10.5 ppm. Approximately 20% of all 409 samples are anomalous. Areas anomalous in arsenic are more widespread than other elements. The Rinconada, the La Guanaca, the Central, and the La Escondida prospects all display arsenic anomalies. The anomalous area in the southern part of Rinconada corresponds to the gold anomalies.

Sb

The background value for Sb is 1.4 ppm. About 14% of all 409 samples are anomalous. Anomalies are distributed in the Rinconada prospect and around the Rinconada area, the La Guanaca prospect, the Central prospect, and the western side of NW trending ridge.

Cu

The background value for Cu is 93.4 ppm. Copper has wider relative dispersion in comparison to the other elements analyzed with 26% of all samples above the anomaly threshold. Four relatively well-defined anomalies are seen in the La Guanaca, the Rinconada, the Central, and the La Escondida prospects, and broad correspond to the silver distribution. The southern area of Rinconada is characterized by several weaker anomalies, in addition to several gold and arsenic. The eastern side of the survey area is also characterized by weak anomalies.

Mo

The background value is 2.6 ppm. Only 5% of all analyses are anomalous and

relatively low. The distribution of anomalies are very restricted. There is a relatively high molybdenum anomaly within the La Guanaca prospect. Weak anomalies are distributed within the La Escondida and Rinconada prospects, and the alteration zone of the Quebrada Emiqueta prospect.

Pb

Lead has a somewhat wider distribution compared to other elements analyzed; 25% of all samples being anomalous.

The area of highest lead concentration is within the Rinconada prospect. Other anomalies are distributed in the Central and La Escondida prospects. No anomalies were detected in the La Guanaca prospect.

Zn

The background value for Zn is 80 ppm. About 30% of all samples are anomalous. Areas of high concentration are distributed within the Rinconada, Central, and La Escondida prospects. There are weak anomalous areas in the southwestern area of the Rinconada, and the eastern of La Guanaca prospect. As is the case with Pb, no anomalies were detected in the La Guanaca prospect.

2-4 Discussion

The distribution of geochemical anomalies with respect to location and element are summarized as follows:

Location	Anomalous Elements
a. La Guanaca prospect	Ag, As, Sb, Cu, Mo
b. Central prospect	Au, Ag, As, Cu, Pb, Zn
c. Rinconada prospect	Au, Ag, As, Sb, Cu, Mo, Pb, Zn
d. La Escondida prospect	Au, Ag, Cu, Mo, Pb, Zn
e. Quebrada Emiqueta alteration zone	Au, As, Mo
f. Southwestern area of Rinconada (includes south ridge of Rinconada)	Au, As, Cu, Pb, Zn
g. Southeastern area of La Guanaca	Ag, As, Sb, Cu, Pb, Zn

Almost all elements analyzed are anomalous in and around prospects a to e. All 8 elements were found to be anomalous in the Rinconada prospect (c). There are no lead and zinc anomalies but a high concentration of copper and molybdenum is

apparent in the La Guanaca prospect,

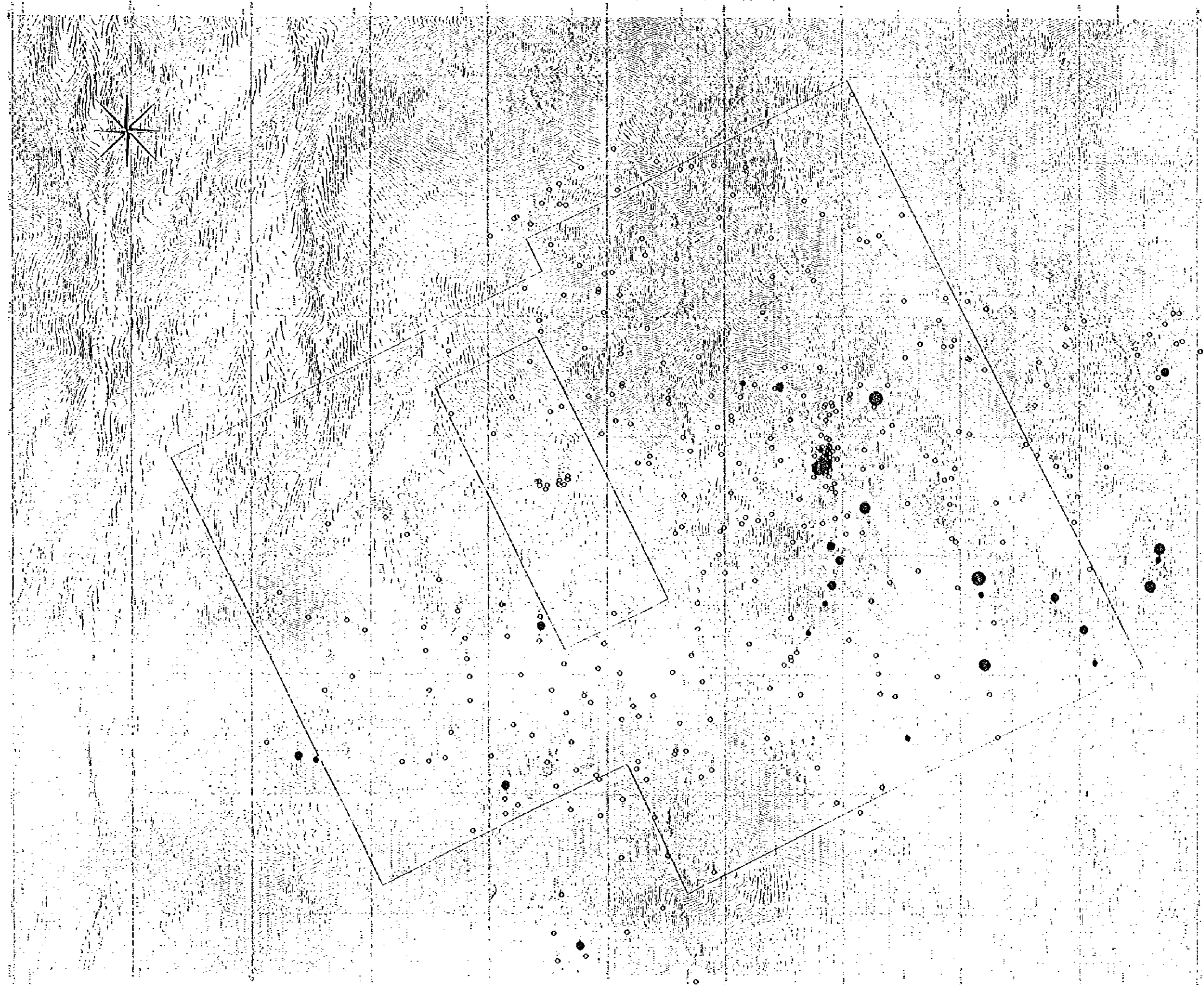
The La Guanaca prospect is characterized by copper and molybdenum anomalies. The Rinconada prospect is characterized by copper, gold, silver, lead, and zinc anomalies. Silver, lead are a little bit higher than the Central prospect.

The type and spatial distribution of geochemical anomalies within the La Guanaca prospect is in general typical of many porphyry Cu style deposits, while the anomalies apparent in the Rinconada and Central prospects maybe interpreted as reflecting the peripheral parts of a porphyry Cu style system.

The southern area of Rinconada is characterized by a relatively high Au anomaly, and when interpreted together with the anomalies in the Quebrada Enriqueta alteration zone, show similarities to what would be expected to be associated with epithermal metal mineralization.

There is no clear spatial relationship between the geochemical anomalies and any apparent geological structure.

GUANACA AU



- AU < 3
- 3 ≤ AU < 12
- 12 ≤ AU < 37
- 37 ≤ AU < 100
- 100 ≤ AU

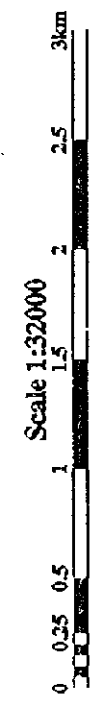
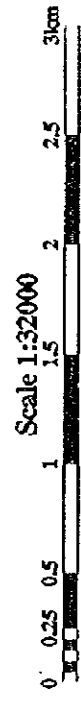
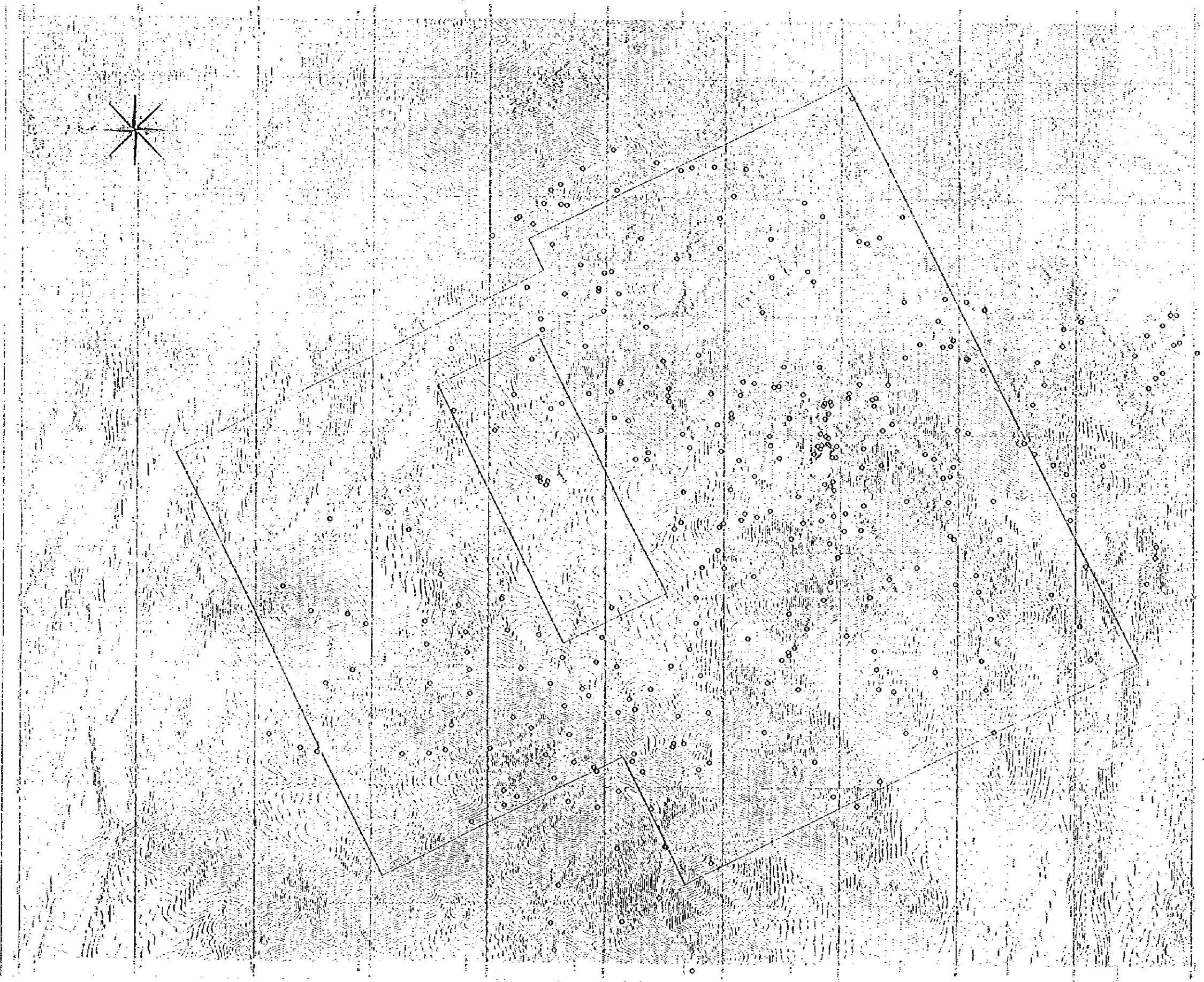


Fig.2-2-1(1) Distribution of geochemical anomalies (Au)

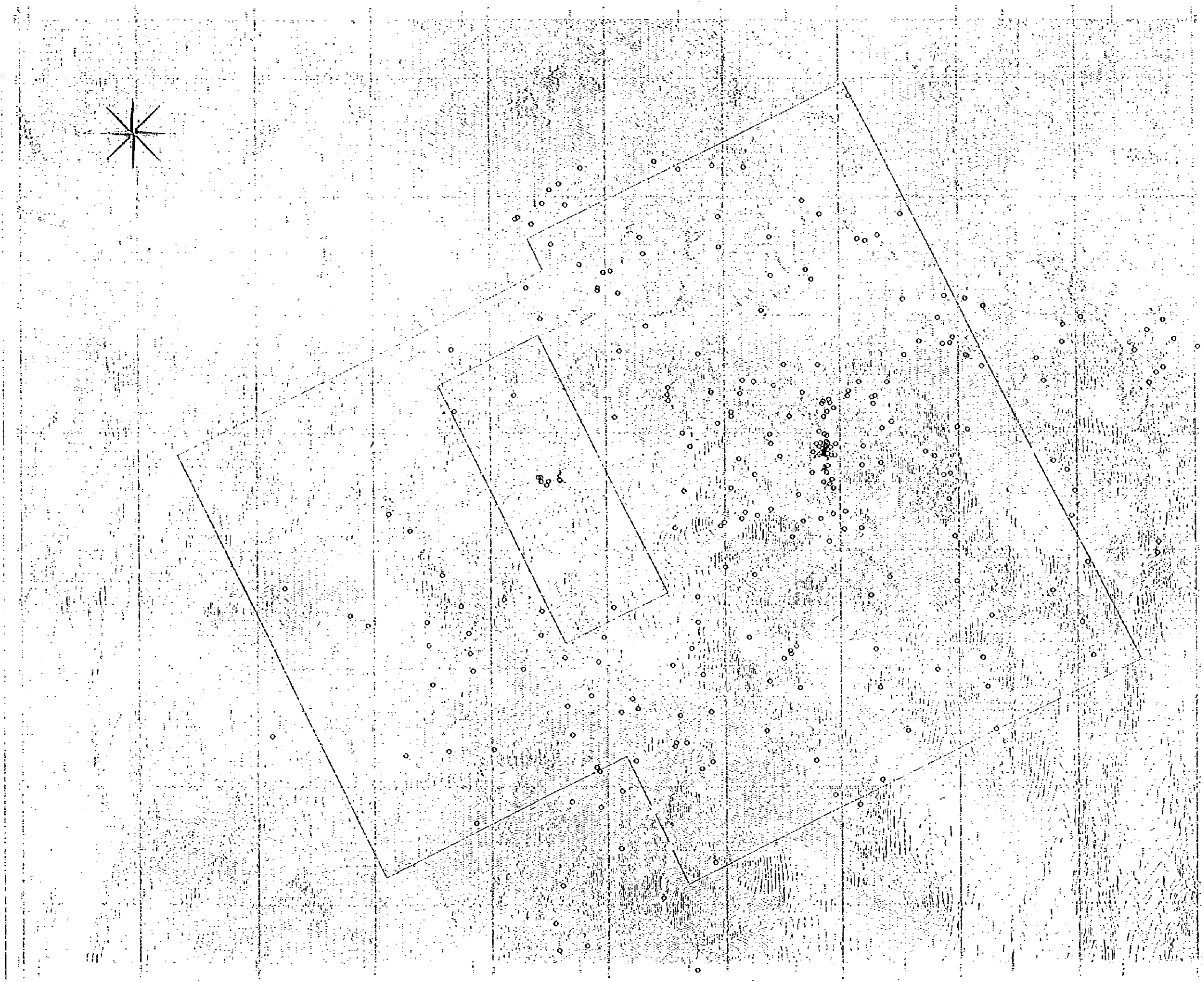
GUANACA AG



- AG < 0.56
- 0.56 ≤ AG < 1.00
- 1.00 ≤ AG < 4.00
- 4.00 ≤ AG < 8.00
- 8.00 ≤ AG

Fig.2-2-1(2) Distribution of geochemical anomalies (Ag)

GUANACA AS

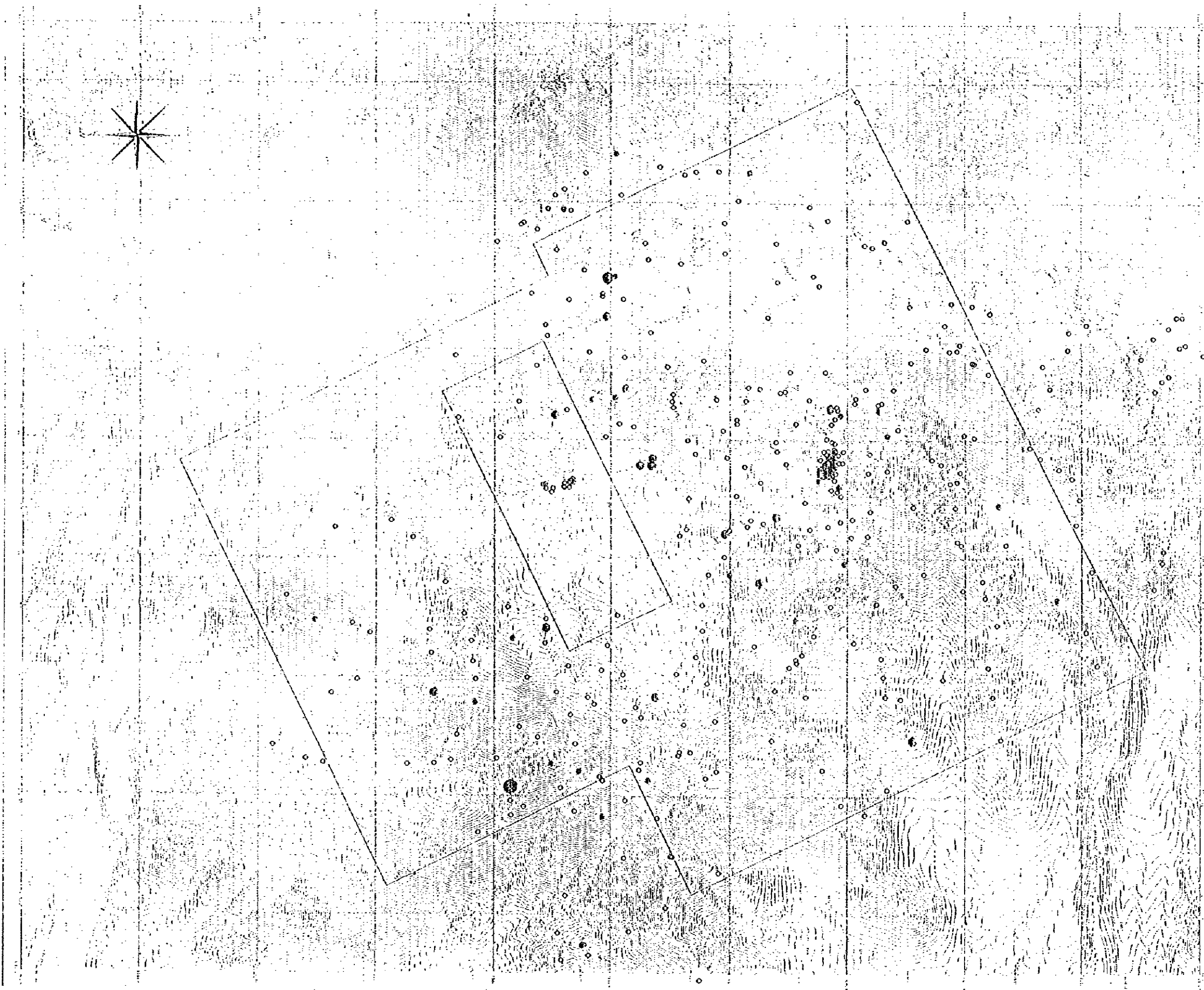


○ AS < 10.5
○ 10.5 ≤ AS < 20.0
○ 20.0 ≤ AS < 30.0
○ 30.0 ≤ AS < 50.00
○ 50.00 ≤ AS

Scale 1:32000
0 0.25 0.5 1 1.5 2 2.5 3km

Fig.2-2-1(3) Distribution of geochemical anomalies (As)

GUANACA SB



- SB < 1.4
- 1.4 ≤ SB < 2.4
- ⊙ 2.4 ≤ SB < 5.0
- ⊗ 5.0 ≤ SB < 8.0
- ⊕ 8.0 ≤ SB

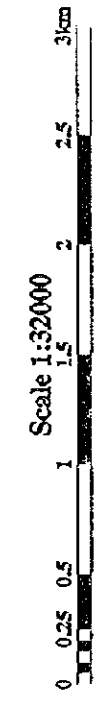
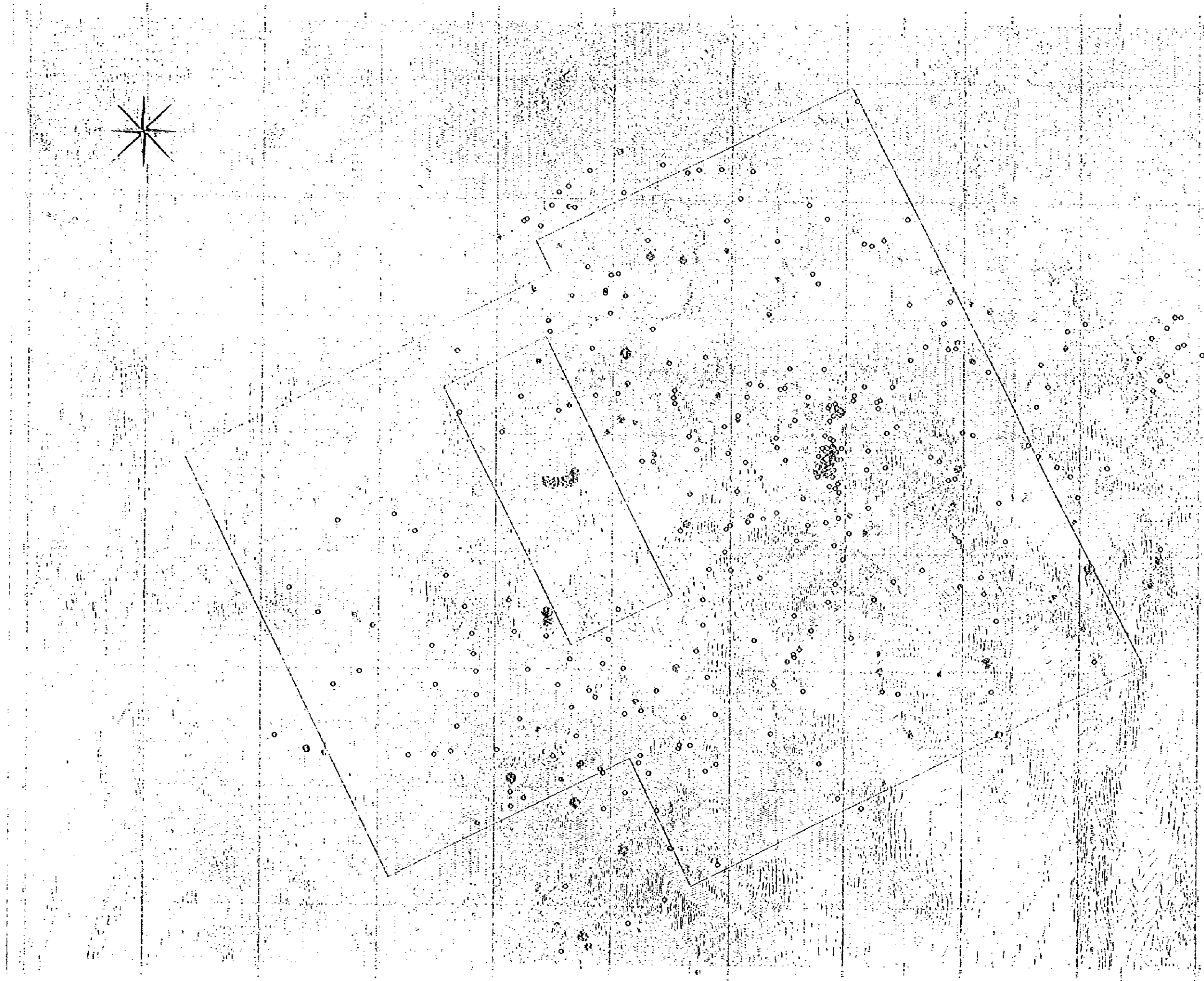


Fig.2-2-1(4) Distribution of geochemical anomalies (Sb)

GUANACA CU



- CU < 93.4
- △ 93.4 ≤ CU < 230.0
- 230.0 ≤ CU < 560.0
- ◇ 560.0 ≤ CU

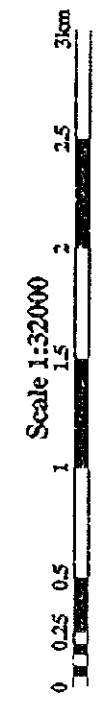
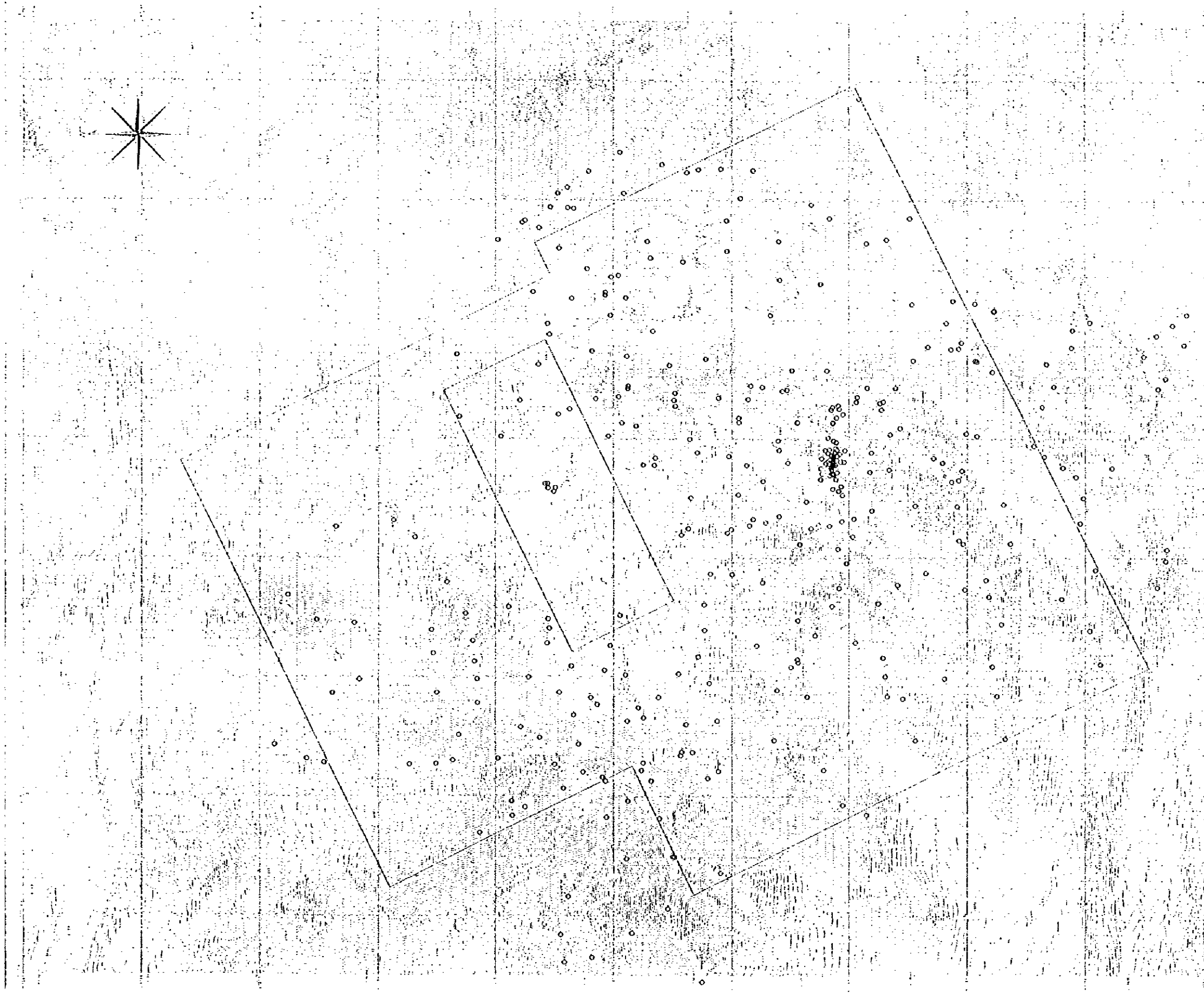


Fig.2-2-1(5) Distribution of geochemical anomalies (Cu)

GUANACA MO

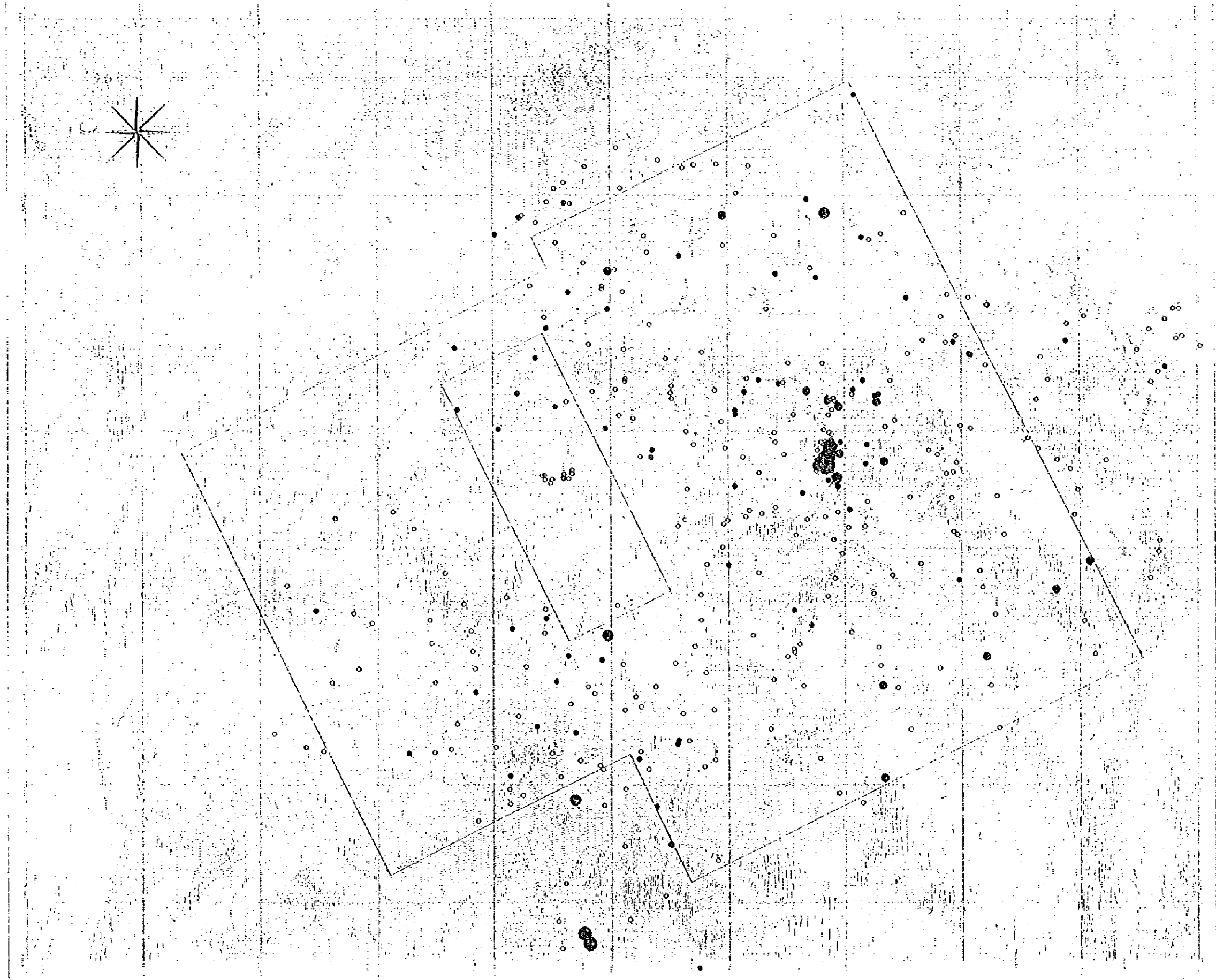


- $MO < 2.6$
- ⊙ $2.6 \leq MO < 5.0$
- $5.0 \leq MO < 15.0$
- ⊗ $15.0 \leq MO$

Scale 1:32000
0 0.25 0.5 1 1.5 2 2.5 3km

Fig.2-2-1(6) Distribution of geochemical anomalies (Mo)

GUANACA PB

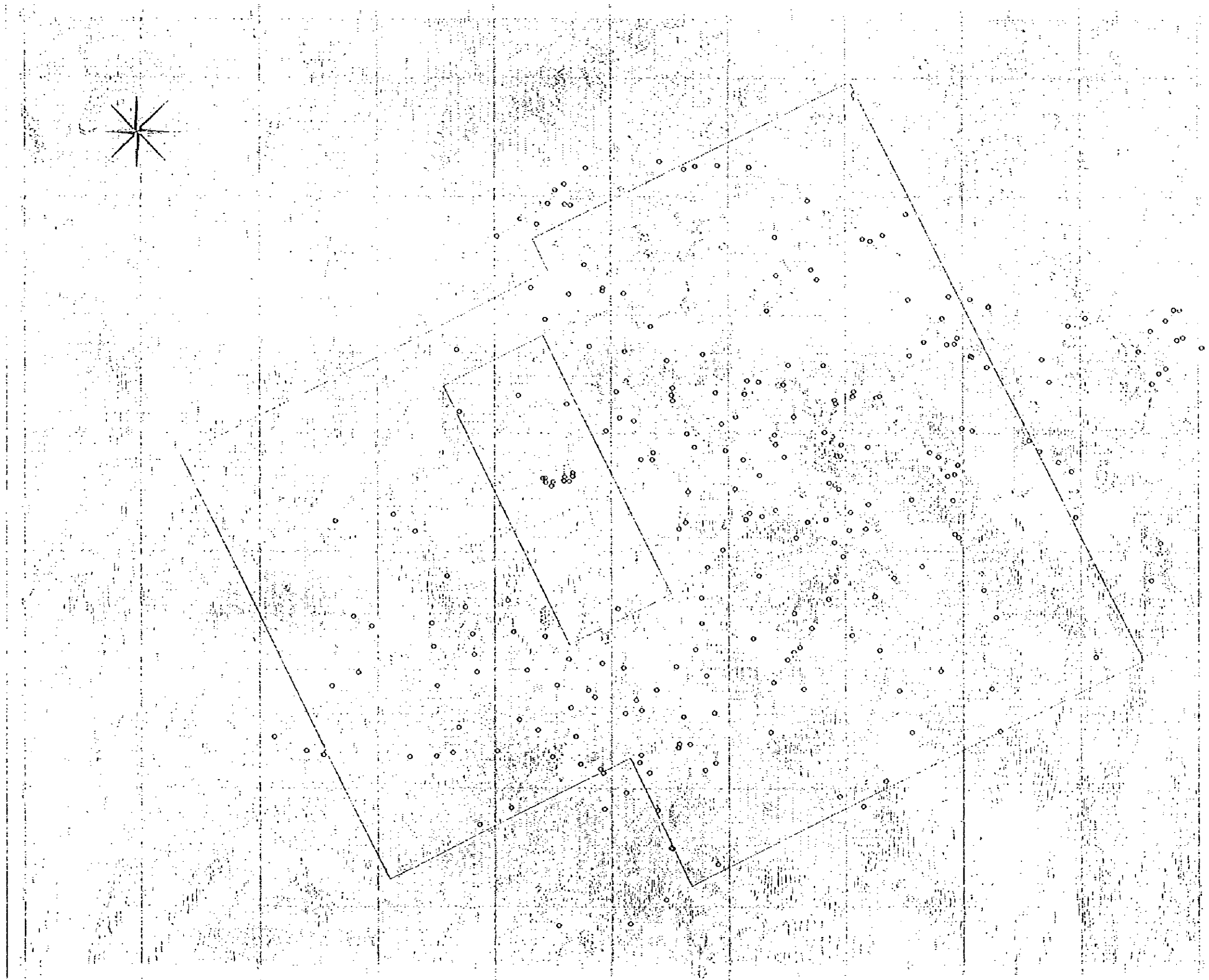


- PB < 12
- 12 ≤ PB < 40
- 40 ≤ PB < 100
- 100 ≤ PB < 300
- 300 ≤ PB

Scale 1:32000
0 0.25 0.5 1 1.5 2 2.5 3km

Fig.2-2-1(7) Distribution of geochemical anomalies (Pb)

GUANACA ZN



- ZN < 80
- 80 ≤ ZN < 150
- 150 ≤ ZN < 200
- 200 ≤ ZN < 300
- 300 ≤ ZN

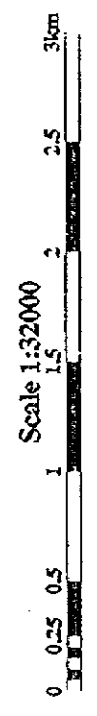


Fig.2-2-1(8) Distribution of geochemical anomalies (Zn)

Chapter 3 Laboratory work

3-1 X-ray Powder Diffraction Analysis

3-1-1 Objective

To establish the alteration characteristics such as alteration mineralogy and zonation, and temperature of hydrothermal activity.

3-1-2 Method

More than 90 samples were collected from outcrops and examined by means of X-ray diffraction.

3-1-3 Results

The results are summarized in Appendix 7. Areas which have undergone hydrothermal alteration are restricted within and around the the prospects surveyed. Samples for X-ray diffraction were mainly collected from the following 3 prospects and outcropping zones of alteration.

- Rinconada Prospect: the sample number is prefixed by a letter
- La Guanaca Prospect : the sample number is prefixed by 1030
- Quebrada Enriqueta alteration zone : the sample number is prefixed by 961025

The samples analyzed by X-ray diffraction were not sufficient in number to delineate any pattern of alteration zonation or hydrothermal temperature structure. It is therefore recommended that further samples be collected and analyzed from the Central Prospect and surrounding areas.

Within the La Guanaca Prospect(see Sheet 4), intense sericitic alteration is observed in the porphyry which is also characterized by disseminated chalcopyrite and pyrite. Samples 103001, 103003, 103005, and 103036 from the porphyry are mainly composed of quartz, sericite, and chlorite. Sample 103036 is waste from the underground workings and has not been effected by supergene alteration. The presence of K-feldspar in this sample indicates that this rock has been subjected to K-silicate alteration. This is supported by the presence of hydrothermal biotite observable during microscopic observation. Samples 103034 and 103035 are from the matrix of the hydrothermal breccia, observable in trenches and near the old pits (Sheet 4), and are

characterized by abundant sericite. Granodiorite 3(Gd3) near the old pit area is partly weak bleached (samples 103015, 103020), and are characterized by patchy smectite that is probably the alteration product from the supergene stage.

All samples from the Rinconada Prospect(see Sheet 4) are characterized by epidote. Samples headed by X and Y are aplitic granites (Ag) scattered away from the pit areas. Other samples were collected from around the pits from where oxide copper was mined. The samples include vein material and host rock near to the veins. Sericite and chlorite alteration are recognized in the host rocks near the veins, in addition, argillized zones near the veins, cerussite ($PbCO_3$), mimetite ($Pb_3(AsO_4,PO_4)_5Cl$), and smectite were identified. These alteration minerals seem to be the product of supergene alteration. In comparison with X- and Y- samples, samples from near the pits are characterized by significant amounts of sericite, chlorite and epidote.

Hydrothermal brecciation and silicification have been identified in the alteration zone of Quebrada Enriqueta. The alteration zone characteristically white in color is mainly composed of sericite/smectite mixed layer clay, while a small amount of sericite is found in the yellowish-brown colored alteration zone. A small amount of kaolintie, smectite, and gypsum were produced during supergene alteration.

3-2 Fluid Inclusion Microthermometry

3-2-1 Objective

Estimate the temperature and salinity of the fluid that responsible for the mineralization by measuring homogenization temperatures and ice melting temperatures of fluid inclusions in quartz veins.

3-2-2 Method

Doubly polished thin sections were prepared from veins sampled from the Central, Rinconada, and La Escondida Prospects, in addition to a few samples from other locations. Approximately 190 fluid inclusions were studied in which homogenization temperatures (T_h) and melting temperatures of ice (T_m) were measured (Appendix 8). Microthermometric measurements were performed by the Odate Chemical Analysis Center using a Linkam TH-600 heating and freezing stage. The salinities were determined from the temperatures corresponding to the disappearance of ice ($T_{m_{ice}}$) and the freezing point depression equations of Potter et al. (1978).

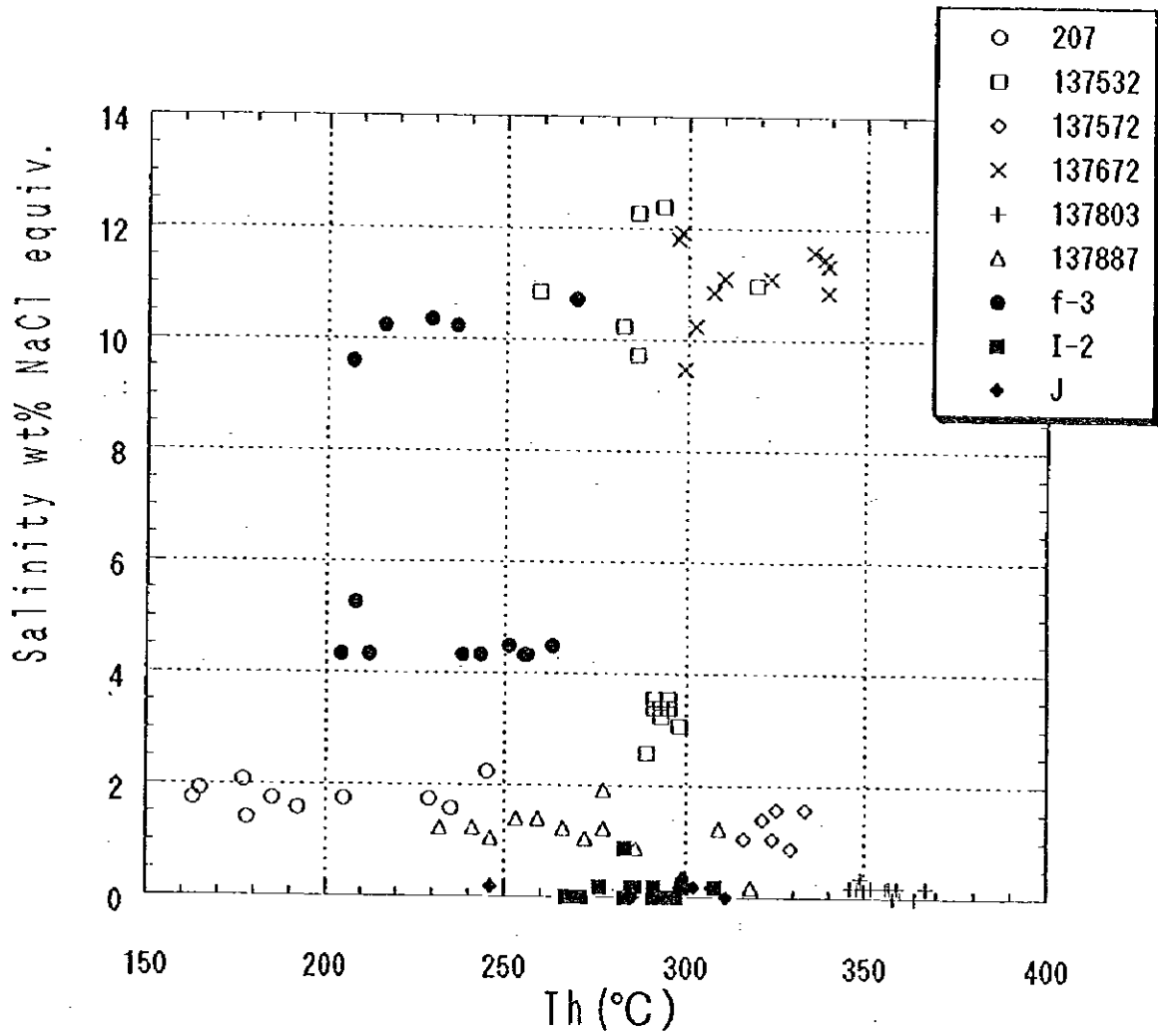


Fig.2-3-1 Th vs. salinity for fluid inclusions, samples 207, La Escondida; 137532 and 137672, Central; 137572, east of Rinconada; 137803, south of Rinconada; 137887, near Cerro El Pimiento; and f-3 ~ J, Rinconada.

3-2-3 Results

The results are summarized in Appendix 8. The relationships between homogenization temperatures and salinities are shown in Fig 2-3-1. Sample locations are summarized as follows:

- Two samples (137532, 137672) from the Central Prospect,
- Three samples (F-3, I-2, J) from the Rinconada Prospect,
- One sample (207) from the La Escondida Prospect,
- One sample (137887) from the southeastern ridge of Cerro El Pimiento,
- One sample (137803) from south of Rinconada,
- One sample (137572) from east of Rinconada, near the 3373.2 m peak.

Fluid inclusions from samples collected from the Central Prospect range in size from 2.5 to 57 μ m. Vapor phase inclusions are common. Vapor phase/liquid ratios display a wide variation. Coexisting liquid-rich and vapor-rich inclusions were identified in the two samples, and provide strong evidence for two-phase conditions due to boiling at the time of formation.

Homogenization temperatures measured for liquid-rich inclusions indicate that quartz and Cu-bearing sulfides crystallized from the hydrothermal fluids within a temperature range of 259° C - 343° C and an average of approximately 300° C.

Relatively high salinities were measured from the two samples mentioned above with values between 9 and 12 wt % NaCl equiv. (Fig. 2-3-1). The salinities measured from sample 137532 display a bimodal distribution, with values falling in the range 10 to 12 wt % NaCl equiv. and 3 to 5 wt % NaCl equivalent. The relative high measured homogenization temperatures and salinities may indicate a relatively significant magmatic contribution to the hydrothermal fluid.

Fluid inclusions from the Rinconada Prospect range from 2.5 to 70 μ m in size. Some liquid phase inclusions are observed and display variable vapor phase/liquid phase ratios. Those variation in the ratios is considered due to necking down. Homogenization temperatures measured for liquid-rich inclusions range from 204° C to 314° C, with an average of 270° C. Salinities are relatively low (around 0 to 0.35 wt % NaCl equiv.; Fig 2-3-1) while one of the samples (f-3) displays a bimodal

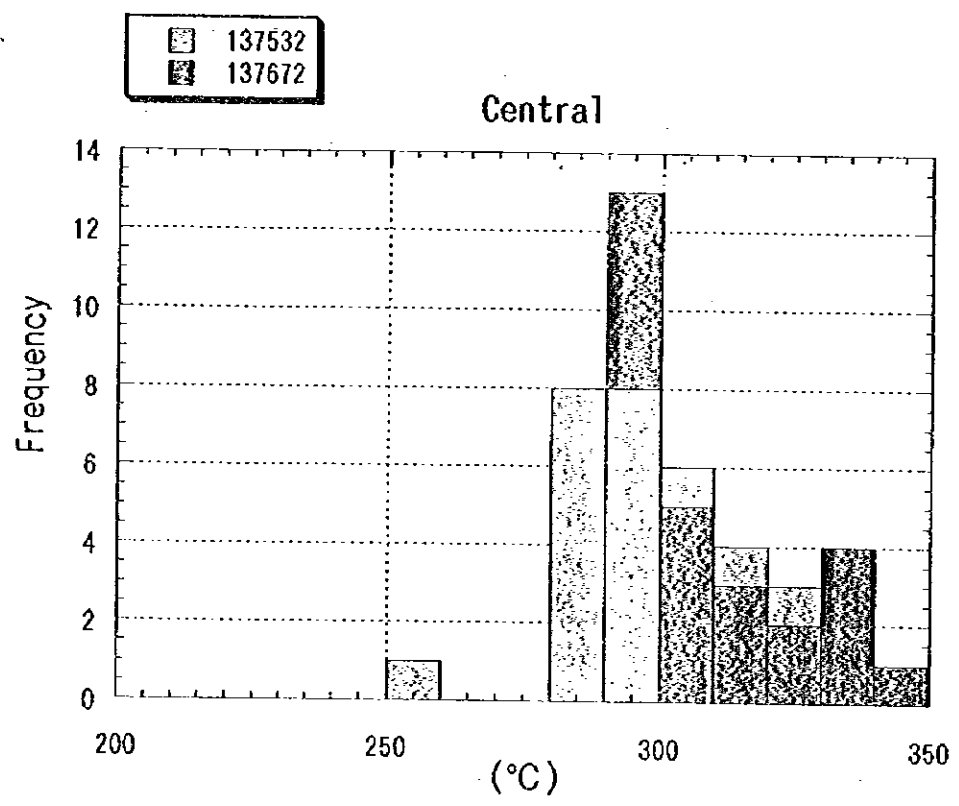
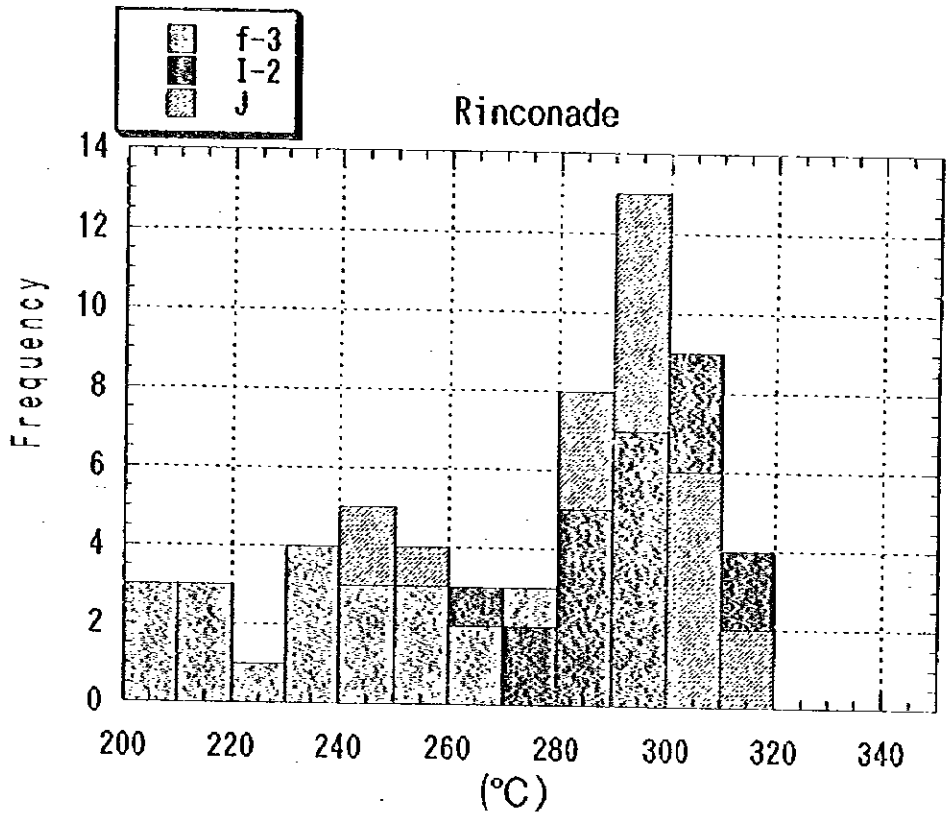


Fig.2-3-2 Homogenization temperatures of fluid inclusions from the Central and Rinconada Prospects.

distribution with peaks centered on 10 and 4.5 wt% wt% NaCl equivalent.

Sample 137803 from south of the Rinconada Prospect was collected from an outcrop approximately 200-250 m higher in elevation than those from the Rinconada Prospect and display variable vapor phase/liquid phase ratios and numerous vapor phase inclusions indicating boiling most probably occurred. Homogenization temperatures are relatively high; 350° C on average while salinities are low; 0 to 0.18wt% NaCl equivalent.

Sample 137887 from the southeastern ridge of Cerro El Pimiento range from 2.5 to 20 μ m in size. Coexisting liquid-rich and vapor-rich inclusions and the existence of vapor-rich inclusions indicate that boiling occurred at the time of vein formation. Homogenization temperatures average 315° C. Salinities are 1.4 to 2.2 wt% NaCl equivalent.

Fig.2-3-2 shows the homogenization temperatures from the Central and Rinconada Prospects. Comparing the data from the two groups, the homogenization temperatures from the Rinconada Prospect have a much wider range and cluster on the lower side compared with those from the Central Prospect. In terms of salinities, fluid inclusions from the Central Prospect are higher than those from Rinconada prospect. Evidence for boiling was observed in the fluid inclusions from the Central Prospect, but were not identified from those of the Rinconada Prospect.

Coexisting liquid-rich and vapor-rich inclusions of primary origin occur in several samples and provide strong evidence for two-phase conditions due to boiling at the time of formation.

3-3 Chemistry of Ores

3-3-1 Objective

Chemical analysis of quartz veins with green copper mineralization were carried out in order to gain estimates of grades and to delineate the nature of mineralization at each of the prospects.

3-3-2 Method

Chemical analysis were carried out by CHEMEX Laboratories using analysis A-30

which analyzes 30 elements. Of these 30 elements, the values of Au, Ag, As, Sb, Cu, Mo, Pb, and Zn are shown in Table 2-3-1. Table 2-3-1 also includes geochemical analyses of samples which have some green copper mineralization. The lower detection limits for each of the elements are as follows: Au: 5ppb, Ag: 1ppm, As, Sb: 10ppm, Cu, Mo, Pb, Zn: 5ppm. The lower detection limits for the geochemical survey samples are shown in Chapter 2.

3-3-3 Results

The results were shown in Table 2-3-1

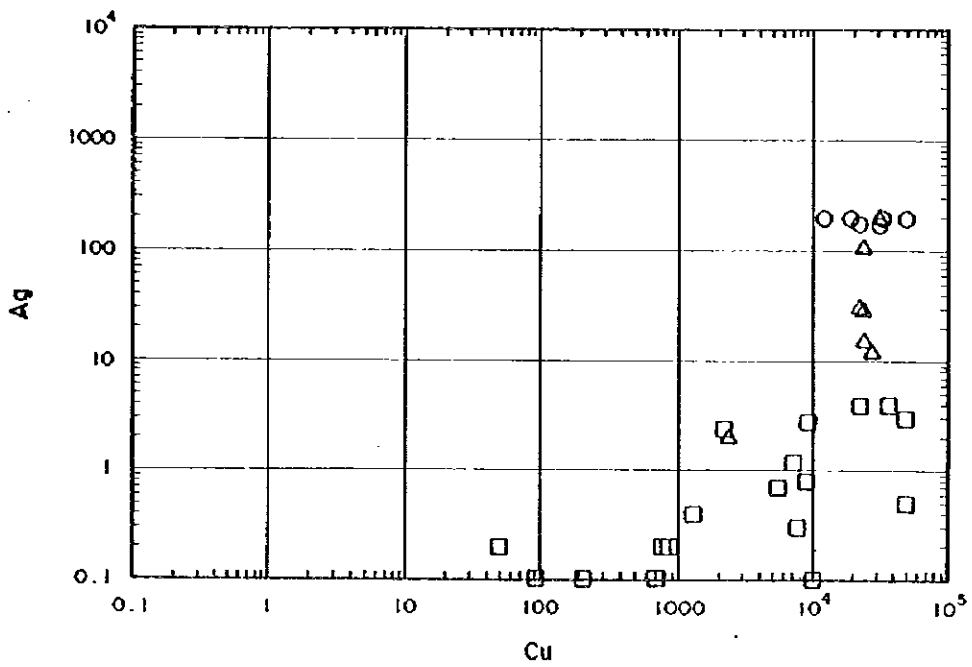
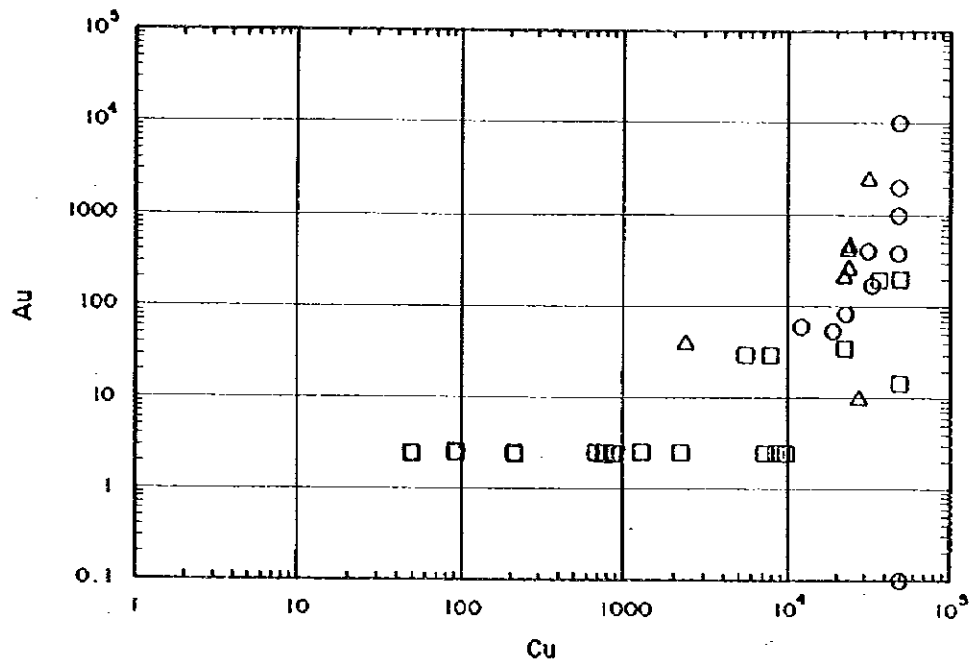
Fig.2-3-3 shows the abundance of each element vs. the abundance of Cu from the La Guanaca, Rinconada, and Central Prospects. A comparison between these prospects indicates the following relationships:

Au: Rinconada \geq Central $>$ La Guanaca
Ag: Rinconada $>$ Central $>$ La Guanaca
As: Rinconada = Central $>$ La Guanaca
Zn: Rinconada $>$ Central $>$ La Guanaca
Pb: Rinconada \gg Central \gg La Guanaca
Sb: Rinconada = Central $>$ La Guanaca
Mo: Rinconada \leq Central \leq La Guanaca
Cu: Rinconada \geq Central \geq La Guanaca

The above relationships are consistent with that of the geochemical anomalies discussed in Chapter 2. Enrichment of Cu and Mo is found in the La Guanaca Prospect and it is considered to have potential for porphyry copper mineralization. In the Rinconada and Central Prospects, besides copper, Au, Ag, Zn, and Pb are enriched. These tendencies may indicate that these two prospects are characterized by a peripheral zone of porphyry copper mineralization (e.g. Lowell and Guilbert, 1970; Lang and Eastoe, 1988; Ortiz et al., 1986; Thompson, 1993; Titley, 1993). In comparison between the Rinconada Prospect and the Central Prospect, the former displays a much higher enrichment in Au, Ag, and Pb. In terms of Mo, the Central Prospect displays a little higher concentration than the Rinconada Prospect. This tendency may indicate that the Central Prospect is nearer to the center of porphyry copper mineralization than the Rinconada Prospect. Greater enrichment of Pb in the Rinconada Prospect is consistent with the results and observation of polish sections and X-ray diffraction of samples from this prospect as galena, cerussite, and mimetite

Table 2-3-1 Chemical analysis for the mineralized samples.

	Au ppb	Ag ppm	As ppm	Cu ppm	Mo ppm	Pb ppm	Sb ppm	Zn ppm	
L a G u a n a c a	103001	<5	0.8	10	8300	151	32	1	10
	103004	30	0.7	18	5500	15	<1	0.8	160
	103005	30	0.3	24	7700	87	20	1.4	238
	103006	<5	1.2	4	7200	10	<1	<0.2	60
	103008	<5	2.8	4	9200	15	<1	0.2	78
	103014	<5	0.4	1	1300	3	<1	<0.2	37
	103015	<5	<0.2	8	690	1	<1	<0.2	44
	103018	<5	<0.2	4	10000	4	<1	0.2	43
	103021	<5	<0.2	1	92	2	<1	<0.2	34
	103022	<5	<0.2	1	210	1	<1	<0.2	33
	103024	<5	0.2	4	850	1	<1	<0.2	34
	103025	<5	0.2	6	800	2	2	<0.2	65
	103026	<5	0.2	4	49	1	1	<0.2	28
	103027	<5	2.4	1	2200	1	1	<0.2	38
	R i n c o n a d a	103002	210	3	30	50000	75	30	5
103010		15	0.5	10	50000	275	595	5	220
103023		200	4	80	37200	475	120	5	770
103036		35	4	10	22600	2.5	15	5	205
137510		2430	200	50	32600	2.5	45000	5	780
L a E s c o n d i d a	A-1	385	200	360	50000	2.5	2710	5	320
	C	405	175	5	31700	2.5	565	5	620
	D-1	1000	200	50	50000	10	2540	5	1610
	E-7	85	179	200	22800	2.5	1650	5	80
	F-6	170	200	550	33300	2.5	50000	260	1445
	H-5A	2000	200	4100	50000	5	44700	570	1130
	H-5B	60	200	910	12110	2.5	10930	10	1435
	J	0	200	180	50000	15	50000	10	435
	K-4	55	200	70	18710	2.5	11630	5	615
	N-3	10000	200	2060	50000	2.5	50000	5	355
C e n t r a l	O-3	390	200	900	50000	110	8930	10	385
	96102808	9600	39	10	27500	5	2830	5	860
	96102811	2730	24	380	14350	25	30000	40	34300
	96102812	240	10	40	38700	2.5	17260	5	1590
	96102818	115	100	50	50000	10	5590	5	2260
C e n t r a l	96102818E	85	95	50	25600	5	3480	5	1155
	137672	40	2	2460	2360	30	4950	5	255
	137676	275	107	20	24400	2.5	60	5	135
	137532	10	12	50	28200	5	510	10	30
	137534	465	15	990	24400	5	2330	5	135
	137530	215	30	130	22700	15	145	5	125
137538	430	29	280	24200	115	610	30	350	

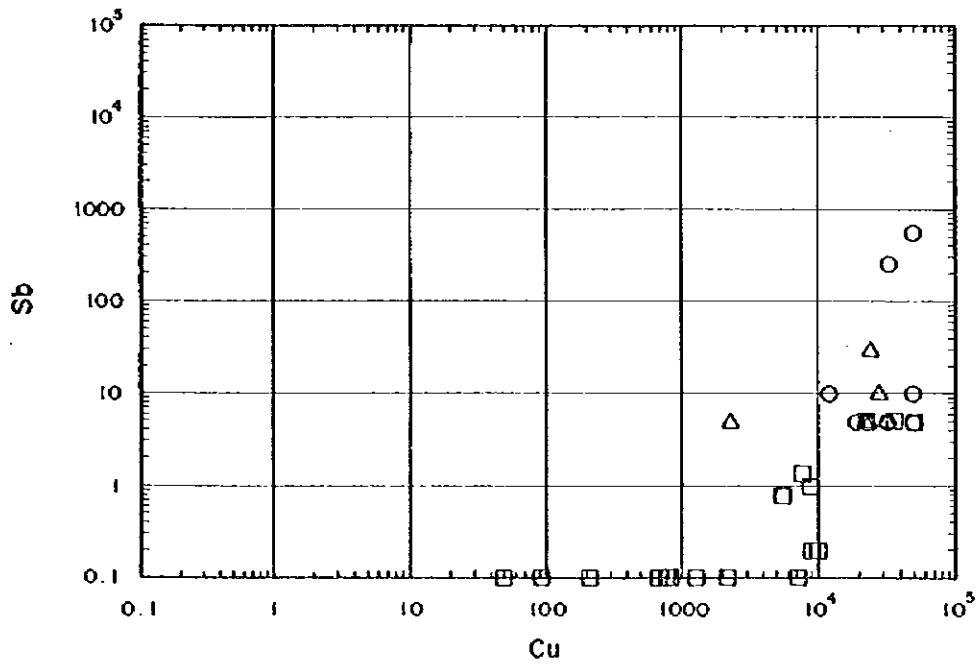
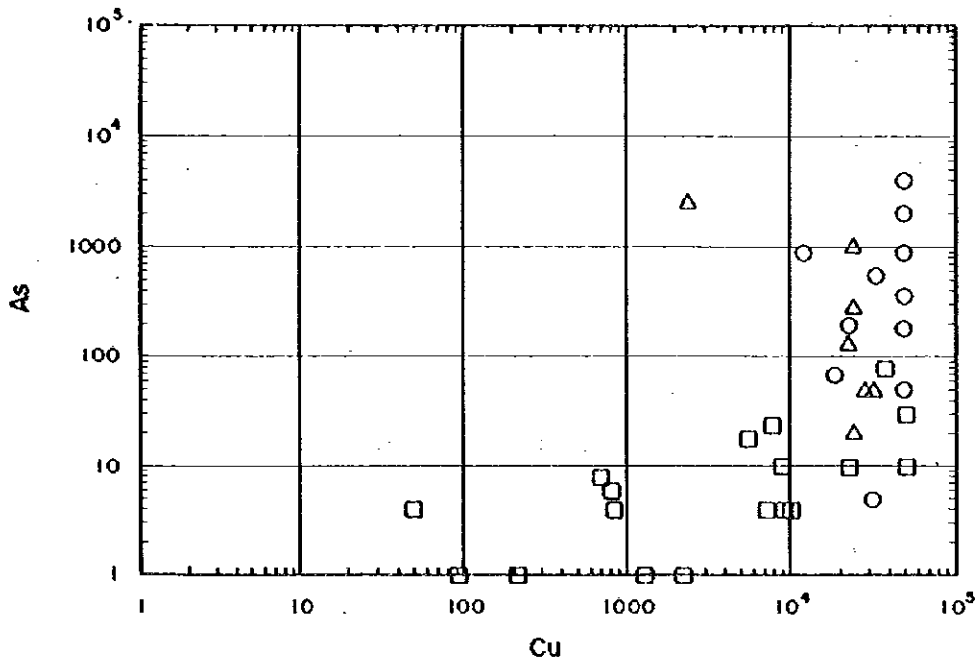


○ Rinconada

△ Central

□ Lo Guanaco

Fig 2-3-3(1) Concentrations for selected elements in mineralized samples from the La Guanaco, Central, and Rinconada Prospects.



- Rincónada
- △ Central
- La Guanaco

Fig 2-3-3(2) Concentrations for selected elements in mineralized samples from the La Guanaco, Central, and Rincónada Prospects.

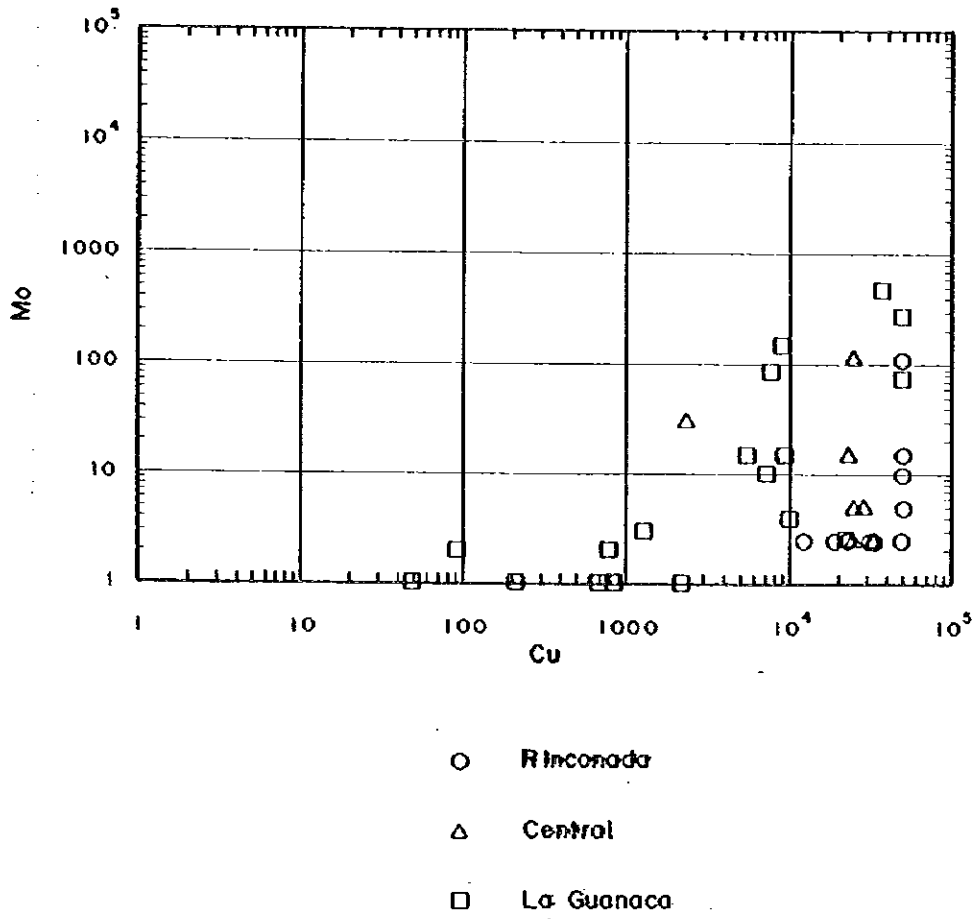
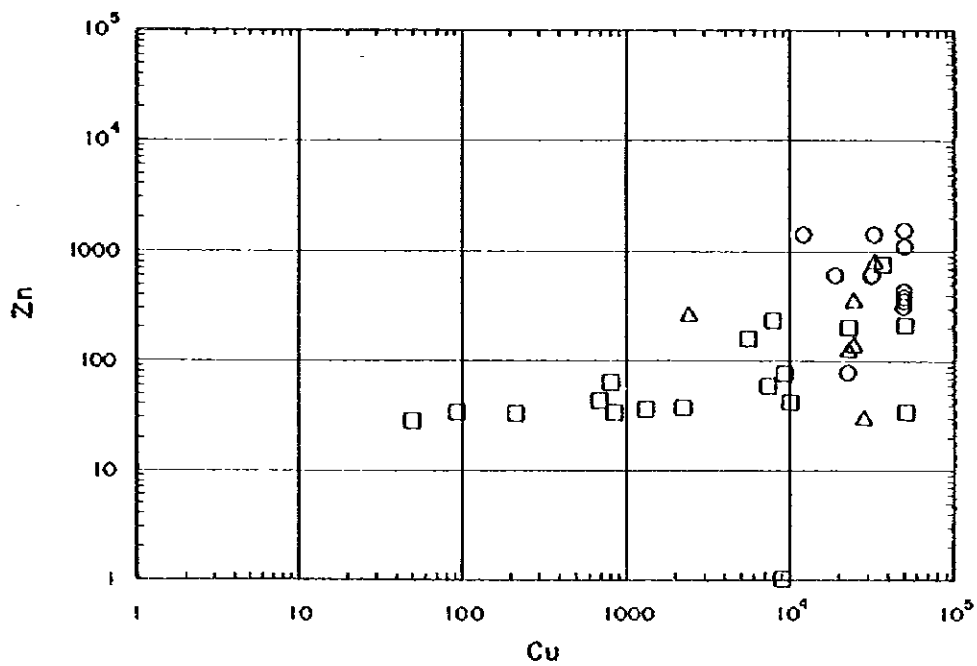
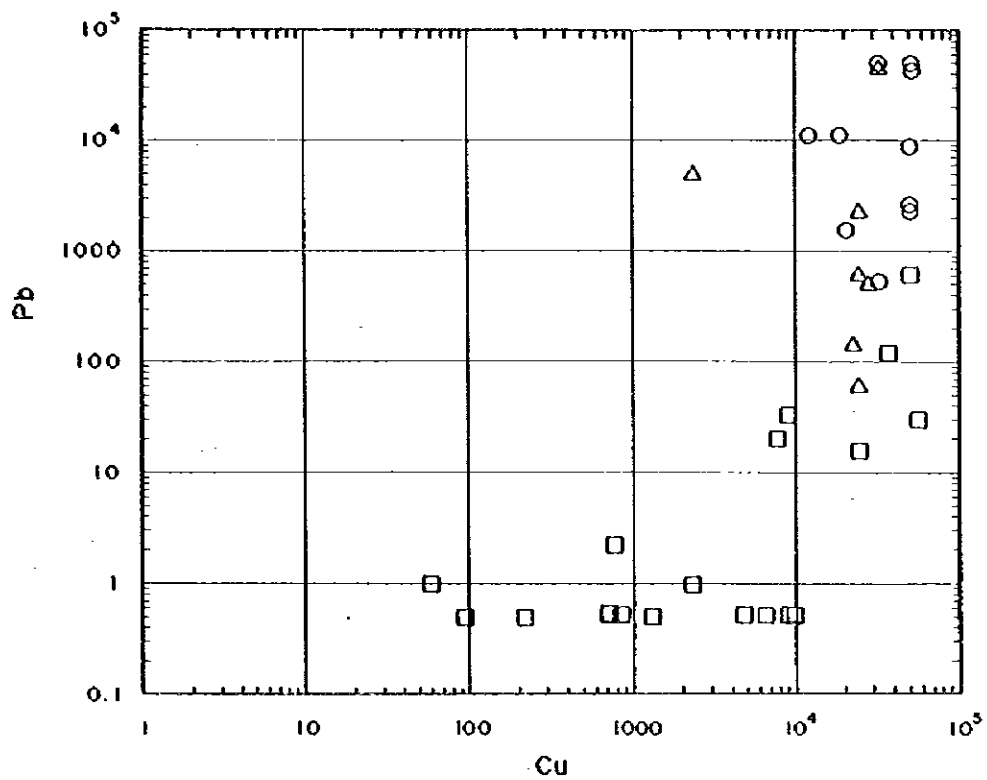


Fig 2-3-3(3) Concentrations for selected elements in mineralized samples from the La Guanaca, Central, and Rinconada Prospects.



- R Inconada
- △ Central
- La Guanaca

Fig 2-3-3(4) Concentrations for selected elements in mineralized samples from the La Guanaca, Central, and Rinconada Prospects.

were identified in veins and altered rocks.

3-4 K-Ar Dating

3-4-1 Objective

K -Ar age determinations were carried out in order to establish the age of the mineralization in the Survey area and any outcropping igneous rocks that may be related to the same event.

3-4-2 Method

Age determinations were carried out by two organizations; Teledyne and the Hiruzen Institute for Geology and Chronology.

3-4-3 Results

The results are shown in Table 2-3-2

[Age of mineralization]

Two sericite samples (137672, e-3) from the Central and Rinconada Prospects were separated from veins that exhibited green copper mineralization. One sericite sample (103034) from the La Guanaca prospect was separated from the matrix of the hydrothermal breccia zone. Sericite 103034 from the La Guanaca prospect gave an age of 43.9 ± 1.1 Ma. The age from sample 137672 can not be used in the discussion as it was not possible to collect a pure sericite sample. The sericite from the Rinconada Prospect (sample e-3) gave an age of 45.6 ± 1.2 Ma and 46.0 ± 1.2 Ma. Thus the mineralization of these prospects occurred almost at the same time during the Middle Eocene.

Comparison between the age of the sericite from the La Guanaca prospect and that from the Rinconada prospect, the latter is a little bit older than the former. This could be explained as reflecting different stages during a single magma-hydrothermal event. The age of the sericite from the Rinconada prospect may indicate an early stage of magmatic-hydrothermal activity, that may correspond to the prophylic alteration. Through the main stage of a porphyry copper mineralization, in the waning stage of the magma-hydrothermal activity, hydrothermal brecciation could have occurred in the La Guanaca prospect. The age of the mineralization of the Survey area is older than that of the El Salvador deposit (41Ma; Gustafson and Hunt, 1975). The age of

Table 2-3-2 K-Ar age of sericite and rock samples

Sample No.	classification on the geological map	K-Ar geological age (Ma)	K(wt%)	⁴⁰ Ar rad (10 ⁻³ cc/g)	Air cont (%)	comment
255	Ga	42.3±2.1	4.3	0.715	78.6	Whole Rock *
137783	Dpf	42.6±2.1	4.7	0.796	75.8	Whole Rock *
137620	M	47.3±2.4	4.66	0.772	82.5	Whole Rock *
137796	Gd1	42.1±2.1	3.09	0.575	86.3	Whole Rock *
137930	Dpf		3.09	0.576	58.9	Whole Rock *
137515	Gd3		2.7	0.447	58.6	Whole Rock **
96110422	Md		2.71	0.449	60.2	Whole Rock **
96102405	Rd				60.3	Whole Rock **
96110418	Ag					Whole Rock **
103034	sericite La Guanaca	43.9±1.1	4.370±0.087	0.753±0.013	37.3	sericite mineral separation **
137672	sericite Central	32.84±0.75	1.597±0.034	0.2182±0.025	14.4	sericite mineral separation **
e-3	sericite Rinconada	45.6±1.2 46.0±1.2	5.440±0.109	0.974 0.984	36.7 36.1	sericite mineral separation **

notice

1. Decay constant of Steiger & Jaeger(1977) is adopted

$$\lambda_e = 0.581 \times 10^{-10} / Y$$

$$\lambda_\beta = 4.962 \times 10^{-11} / Y$$

2. Ratio of ⁴⁰K in X is ⁴⁰K/^K=0.01167 atom%

3. Assumption of measurement error is Nagao et al.(1984)

*:Teledyne Ltd. Analyzed
**:Hiruzen Institute for geology and chronology

mineralization of the El Salvador deposit is 41Ma (Gustafson and Hunt, 1975) slightly younger than that of the Survey area.

[Age of rocks]

Almost of the rock samples used for whole-rock age determinations are altered to varying degrees. An exception is sample 137515.

Sample 255 is a Green andesite(Ga). All phenocrysts of plagioclase are altered to sericites and epidotes, while phenocrysts of pyroxene and hornblende are also altered to chlorites and epidotes. Therefore the 42.3 ± 2.1 Ma age of this rock reflects the alteration age.

Sample 137783 and 137930 are lapilli tuff (Dpf). This horizon is between the Llanta andesites (Ba) and the Green andesites (Ga). The Ocoitic andesite (Oa) may intrude between the lapilli tuff (Dpf) and the Green andesites (Ga). In this situation, the determination of the age of lapilli tuff (Dpf) constrains the age of volcanic activity in the Survey area. Collection of a fresh sample of this unit was not possible. The samples measured are strongly altered with ages of 42.6 ± 2.1 Ma. These should also be considered as alteration ages and are the same as that of sample 255 (Ga).

137620 is belongs to a Quartz Monzonite(M) from the northwestern area. Plagioclase are partly altered to sericite, while most of biotites are altered to chlorite. Many hornblendes however are free of alteration to biotite. Therefore the 47.3 ± 2.4 Ma age is most probably younger than the true age. Comejo et al.(1993) report a K-Ar age of 63 ± 2 Ma for this rock.

Sample 137796 is a Granodiorite1(Gd1). This rock is thought to be youngest granitic rocks from its occurrence in the Survey area. Felsic minerals are not altered, but mafic minerals such as hornblende and biotite are altered to chlorites. This measured age of 42.1 ± 2.1 Ma also indicates the age of alteration.

Sample 137515 is Granodiorite3(Gd3). This rock is the host rock of the mineralization in the La Guanaca and Central Prospects. Under the microscope, some biotites are altered to chlorite, however few other minerals are altered. The age of this sample would indicates the age of this rock. The data are not in available at this time. This rock grades into Granodiorite4 (Gd4). The K-Ar age of the Gd4 sample is about 48 Ma

(Comejo et al., 1993).

Sample 96110422 is a Quartz Monzonite(Md). Plagioclases are partly altered to sericites and epidotes. Pyroxene and hornblende are altered to chlorite, epidote, and opaque minerals. Sample 96110418, an aplitic granite (Ag), has also been subject to alteration. The aplitic granite is the host to the vein mineralization in the Rinconada Prospect. However, the data are not in available at this time.

96102405 is a rhyolitic volcanic breccia(Rd). This rock is believed to intrude the Green anesite (Ga) from its occurrence (Fig.2-1-9), however, the sample is silicified and hydrothermal biotites were produced. The age of the sample shows the alteration age. The data are not in available at this time.

CHAPTER 4 GEOPHYSICAL SURVEY

4-1 Purpose of Geophysical Survey

The purpose of geophysical survey is to elucidate relation between Resistivity structure, IP anomaly and mineralization of porphyry copper in the survey area. Major factors we considered for choosing survey methods for this project are as follows:

- ① There are two mineralized zones of copper oxide, La Guanaca and Rinconada de Villanueva, and it was confirmed that disseminated sulfide ore presented in La Guanaca.
- ② As the survey area is overlain by gravels, it is difficult to extract a promising area from geological survey results.
- ③ There are very weakly altered zones of low apparent resistivity in the survey area.
- ④ The survey area is underlain by granite and andesite which will present high resistivity.
- ⑤ As the survey area belongs to desert with a little soil, it is expected that grounding resistivity is very high.
- ⑥ As it is very steep topography, measuring equipment and system must be compact and portable.
- ⑦ There is only one way for to the center of the survey area from north to south, but not through out to the southern part.

After consideration, Time-domain IP method was adopted.

Typical rocks and ores were sampled in the survey area and Resistivity and chargeability of samples were measured in the laboratory. These results were refereed with field data.

Table 2-4-1 shows specifications of the survey and equipment used for the survey.

Table 2-4-1 Specification of Geophysical survey

Length of survey lines	60.0 km
Number of survey lines	12 lines
Method of measurement	Time domain IP
Electrode	Dipole-dipole array
Electrode spacing(a) :	200m
Laboratory Measurement	45 samples

Table 2-4-2 List of equipment and materials

Equipment	Maker	Model	Speticication	Amount
Transmitter	Iris instruments	VIP3000	Output max.: 3000V, 5A, 3000W	1
Engine Generator	Kubota	AE2200	50Hz , 220V ,Max. power: 1.9kW	1
Receiver	Scintrex	IPR-12	8 channel, input range: 50 μ V~ 14V	1
Current Electrode			Buried copper net	20
Potential Electrode			Non Polarizing Porous-pot electrode, Cu-CuSO ₄	14
Cable	Cocesa	Cable Tac	No.18 AWG 300V	1
Positioning Device	Magellan	Meridian XL	Accuracy(potioning: 15rms(2D mode),speed:+,- 0.1knots)	1
Measuring Compass	Ushikata		Pocket Compass, 100m Esron Tape	3
Communication Device	Kenwood	TH-42	Output : 600mAhW, Battery : 12V	11

4-2 Method of Geophysical Survey

4-2-1 Survey Lines Arrangement and Survey of Topography

Major factors we considered for arranging survey lines for the survey area are as follows:

- ① As the survey area has a near rectangular out shape, survey line parallel to the side enable the survey to take data wide and deep.
- ② Mineralized zones are arranged on a line from north to south.
- ③ There is only one way for to the center of the survey area from north to south, but not through out to the southern part.

After consideration, the survey lines were arranged near parallel to the side of the survey area(N62E-S62W).

Survey of topography along survey lines are set from geodetic survey base point near La Guanaca. Coordination of base point was read on a map

of existing documents. Survey of topography was carried out with a measuring tape and a pocket-compass. Spacing between survey stations is 200 meters.

Fig.2-4-1 shows the location of survey lines and stations.

4-2-2 IP Survey

1) The principle of IP method

Induced polarization method, abbreviated as IP method, is a method to measure electrical polarization of rocks in the ground. When the electric current is sent into the earth, various electro-chemical phenomena occur in the medium which composed the earth. Two phenomena are measured in IP survey as follows.

[Over Voltage Effect]

An electric current leads superficially electric double layer on the surface of sulfide and metal conductors. An electric discharge occurs to opposite direction as switching off an electric current. This phenomenon is occurred by the complex effect of ion and electron conduction. This Phenomenon results from the mineral with an electron conductivity and is an object of IP survey.

[Normal Effect or Background]

Polarization occurs by sending an electric current in ordinary rocks. This phenomenon results from mainly membrane polarization caused by a small quantity of clay minerals mixed in rocks. The membrane polarization of montmorillonite is the biggest of all of the various clay minerals and that of kaolinite is small. The membrane polarization is maximum when there is 5% clay minerals in volume. However, a membrane polarization decreases when the capacity ratio is larger or smaller than 5%. The maximum membrane polarization is approximately 2% in frequency effect when there is 5% montmorillonite in volume. This is extremely small compared with above-mentioned Over Voltage Effect in the sulfide minerals.

2) Measuring method of IP phenomena

There are two ways of measuring IP phenomenon, as time-domain and frequency-domain. If we measure IP effect of extremely wide range of frequencies and long time range of transient potential decay, frequency-domain measurement and time-domain measurement are equivalent through Fourier transform. Economically it is not feasible to measure IP phenomenon in very wide range of frequencies. Recently, advancement of computer technology made time domain measurement, which contains more

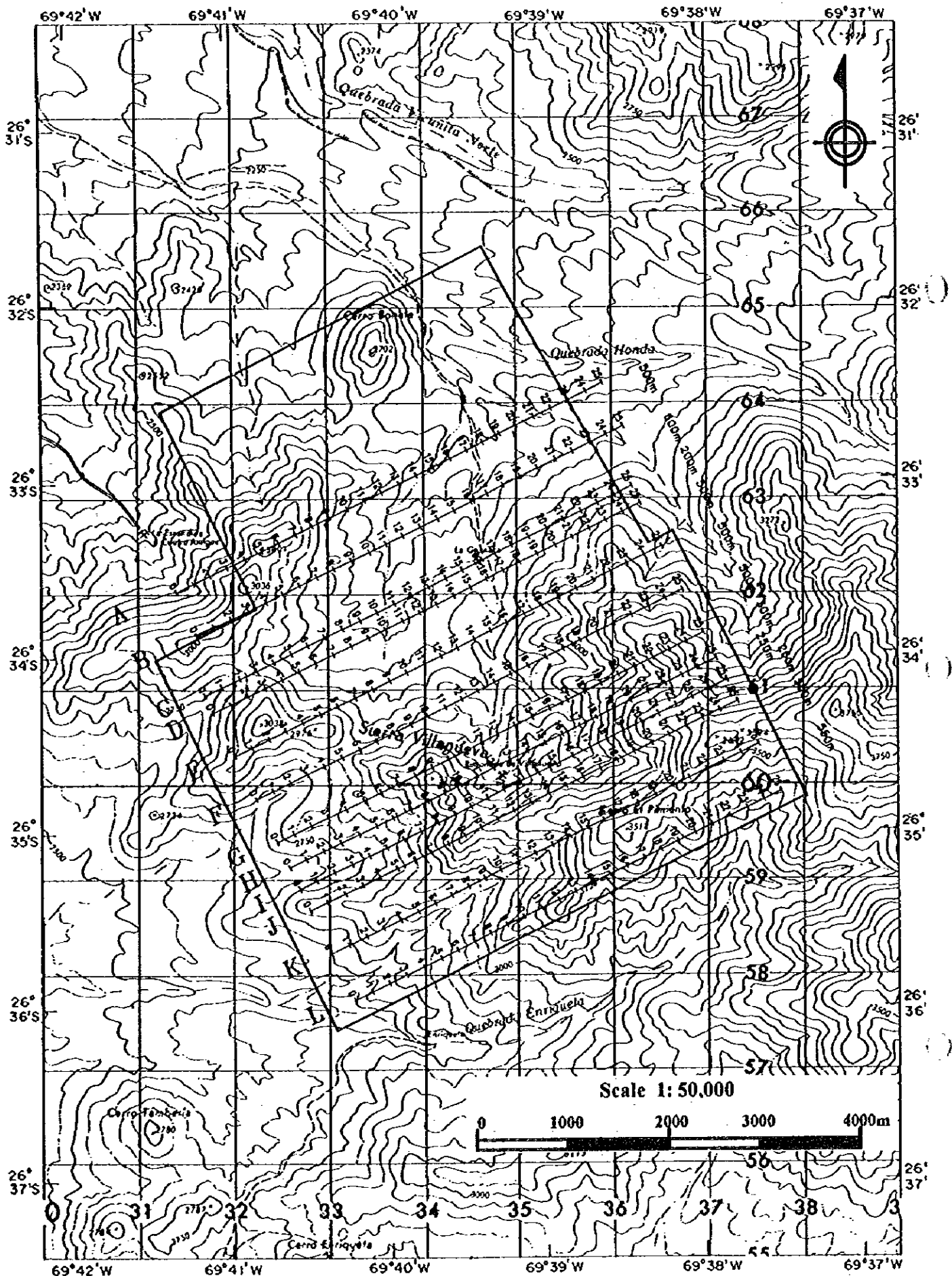


Fig.2-4-1 Location of geophysical survey lines

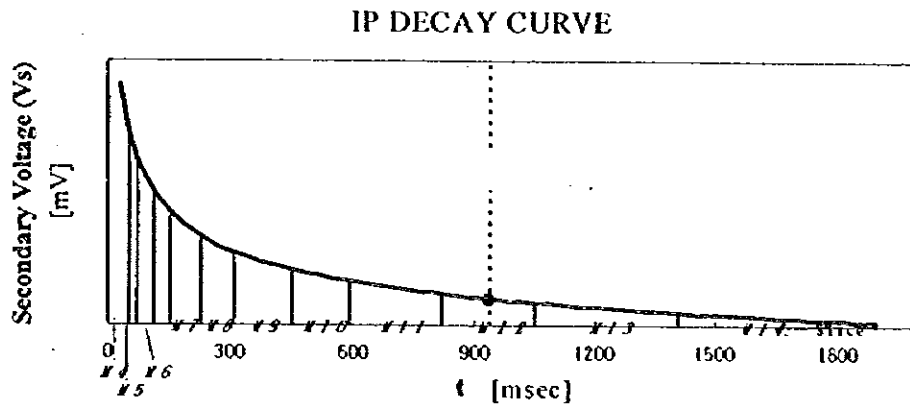


Fig.2-4-2 Concept of IP method

Table 2-4-3 List of sampling time

Slice #	4	5	6	7	8	9	10	11	12	13	14
Width(msec)	20	40	40	80	80	140	140	230	230	360	360
Mid-point(msec)	60	90	130	190	270	380	520	705	935	1230	1590

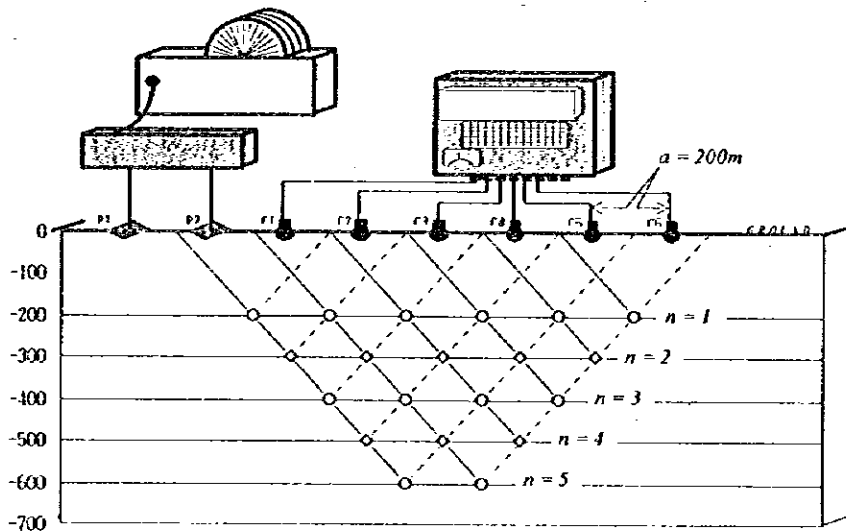


Fig.2-4-3 Configuration of dipole-dipole array

information, more popular. This survey used time domain measurement. The configuration of measurement is shown in Fig.2-4-2.

In the time-domain IP method, an intermittent direct current (on/off 2.0 sec) is transmitted into the ground through a couple of current electrode C1 and C2. Then Two kinds of data are measured through a couple of potential electrode P1 and P2. One is the primary voltage(V_p) just before turning off transmitting current, the other is the secondary voltage(V_s) during the time(t_1 to t_2) after turning off transmitting current. The secondary voltage(V_s) gradually decays to zero after current turned off.

The measured value of IP effect in time-domain IP method is generally termed with chargeability, shown as V_s/V_p [mV/V]. Secondary voltage(V_s) is defined as an integrated V_s on decay curve divided by time(t_2-t_1) as the following equation.

$$V_s = \frac{\int_{t_1}^{t_2} V_s(t) dt}{(t_2 - t_1)}$$

In this survey, we measured secondary voltage(V_s) on decay curve between 40 msec and 1770 msec after turning off transmitting current and chargeability in mid-point 935 msec was adopted to analysis. The concept of measuring method is shown in Fig.2-4-2 and the list of sampling time is shown in Table 2-4-3.

One of major noise source of IP measurement is electromagnetic coupling between cables connecting current electrodes and cables connecting potential electrodes. This survey used dipole-dipole electrode configuration which gives smallest electromagnetic coupling between cables.

Apparent resistivity of dipole-dipole configuration can be calculated by the following formula where electrodes are set along a straight survey line.

$$\rho_a = n(n+1)(n+2) a \frac{V}{I}$$

where : the ratio of the circumference of a circle to its diameter
3.14159....

V: measured potential difference (volt)

I: transmitting current (ampere).

a: electrode spacing (m)

n: electrode separation index.

4-3 Analysis

4-3-1 Method of Analysis

1) Sample measurement

Typical rocks and ores are sampled from the survey area. 45 samples' resistivities and chargeabilities were measured in a laboratory.

3cm to 5cm cubes cut samples were immersed in water for a day.

The resistivity and chargeability of these samples were then measured in the time-domain IP method as same equipment in the field survey.

Table 2-4-4 shows results of sample measurement. Fig.2-4-4 shows relationship between chargeability and resistivity of rocks and ores.

Resistivity of rock samples varies very widely from 169 ohm-m in tuff to 31912 ohm-m in andesite, and chargeability also varies widely from 0.12 mV/V in andesite to 8.23 mV/V in granite.

Aplitic granite, hornblende-biotite granite, biotite-hornblende granodiorite and gabbro or diorite show relatively low resistivity near or less than 2000 ohm-m and high chargeability of about 5 mV/V.

Monzodiorite, aplite, andesite and andesitic pyroclastic rock and ocoita show high resistivity over 10000 ohm-m and low chargeability of about 3 mV/V.

Most of Chrysocolla shows low Resistivity less than 1000 ohm-m and low resistivity of about 3 mV/V.

Disseminated sulfide ore shows low resistivity of 433 ohm-m and high chargeability of 54 mV/V.

Some Chrysocolla shows low resistivity less than 1000 ohm-m and slightly high chargeability of 7.43 mV/V.

Dacitic lapilli tuff or welded tuff and aplitic granite show almost same resistivity to sulfide ore.

There are no other rocks show like as chargeability of sulfide ore. Maximum chargeability of rocks is 7.97 mV/V in dacitic lapilli tuff or welded tuff.

Therefore, resistivity value of sulfide ore which is a target in this survey is located among those of other rocks, but chargeability of sulfide ore exceeds those of other rocks.

It was concluded that analyzed model would be discriminated sulfide ore body from other rocks by the difference of chargeability.

As disseminated sulfide ore generally makes lower resistivity and makes higher chargeability, model resistivity was modified low and model

Table 2-4-4 Results of sample measurement

No	Location	Rock	Resistivity(Ohm-m)		Chargeability(mV/V)	
				Average		Average
27	I 0.0	Tuff-Lapilli Tuff	169	1183	1.1	3.3
31	J 0.0	Tuff-Lapilli Tuff	963		1.5	
26	G 22.0	Tuff ?? or Andesite	1045		8.0	
5	B 0.0	Tuff	2558		2.6	
6	B 2.0	Tuff	286	706	2.7	5.2
34	J 23.0	Tuff	433		5.8	
18	F 0.0	Tuff or Metamorphic Andesite	849		5.8	
1	A 0.0	Tuff	864		6.3	
32	J 10.0	Aplitic Granite	1096		5.5	
33	J 16.0	Aplitic Granite	1268	1590	4.4	6.3
40	L 17.0	Aplitic Granite	1912		8.2	
28	I 9.0	Aplitic Granite	1066	2304	5.7	4.6
29	I 19.0	Aplitic Granite	1098		5.5	
3	A 12.0	Granite	1252		3.6	
7	B 7.0	Granodiorite	2056		2.9	
9	C 7.0	Granodiorite	6047		5.4	
16	E 6.0	Granodiorite	703	703	3.5	3.5
15	E 3.5	Granodiorite	905	10235	4.3	2.9
23	F 22.0	Dyke ??? or Tuff ? - ? -	10418		2.4	
20	F 15.0	Monzodiorite	19382		2.1	
25	G 18.8	Monzodiorite - Granodiorite	13761	13472	0.4	0.8
4	A 18.0	Monzodiorite-Quartz Monzonite	13182		1.2	
12	D 0.0	Quartz Monzodiorite	876	12171	7.7	2.2
21	F 18.5	Monzodiorite	3740		2.1	
36	K 21.0	Monzodiorite	3862		4.0	
19	F 5.0	Diorite ?	3978		1.4	
30	I 25.0	Greenish Andesite	4419		3.7	
35	J 25.0	Greenish Andesite	5124		1.4	
22	F 21.0	Greenish Andesite	9253		2.8	
24	G 6.0	Metamorphic Greenish Andesite	9413		1.0	
38	L 6.0	Greenish Andesite	12272		0.7	
8	C 0.0	Andesite(Formation Llanta)	13024		-0.1	
10	C 19.0	Andesite(Formation Llanta)	13460		1.0	
17	E 25.0	Andesite(Formation Llanta)	18172		1.3	
11	C 22.0	Andesite(Formation Llanta)	20540		0.9	
2	A 7.6	Andesite(Formation Llanta)	21855		2.1	
14	D 25.0	Andesite(Formation Llanta)	22841		0.2	
13	D 22.0	Andesite(Formation Llanta)	31912		4.6	
39	L 10.0	??? Ocoita ??? - ? -	7133	10968	4.0	3.3
37	L 4.0	Ocoita	14802		2.6	
41	La Guanaca	Disseminated Sulphide Ore(Porphritic)	433	433	54.1	54.1
42	La Guanaca	Aplitic Granite Crysocola	143	2247	7.4	3.8
43	La Guanaca	Aplitic Granite Crysocola	338		3.1	
45	J 11.0	Aplitic Granite Crysocola	739		2.2	
44	Rinconada de Villanueva	Aplitic Granite Crysocola	7770		2.4	

chargeability was modified higher in case of less difference between observed data and synthetic data.

On the other hand, less mineral in disseminated rock makes higher resistivity, but sometime not makes lower chargeability. As in resistive rock secondary voltage(Vs) is discharged during long time and resistive rock apparently shows high chargeability out of proportion with its mineral content.

Then mineral content is not estimated by chargeability, and chargeability varies with resistivity of kind of host rocks and their constituent minerals.

2)Simulation

IP survey results are presented as apparent resistivity pseudo-sections and chargeability pseudo-sections along each survey lines. Apparent resistivity is calculated with bent of survey lines being considered.

Based on pseudo-sections, resistivity and chargeability structures were modeled on two-dimension along each lines. Those models were calculated by forward program and compared with obtained data. Models were modified to decrease differences between observed data and synthetic data, and then models were calculated again by trial and error up to get models of minimum differences between observed data and synthetic data. Inversion program was also used partly. A software used in analysis was RESIX IP2DI by Interpex Limited, USA. RESIX IP2DI calculates the theoretical response using the finite element routine developed by Rijo(Rijo,1977) and the 2-D inversion of free parameters based on the Inman ridge regression algorithm(Inman, 1975).

The results of inversion are presented as resistivity and chargeability sections along 12 survey lines. Panel diagram is drawn to show relation of resistivity distribution along each line.

4-3-2 Results of Analysis

Apparent resistivity pseudo-sections and maps are shown in Fig.2-4-5. Chargeability pseudo-sections and maps are shown in Fig.2-4-6.

While chargeability values are almost 2 to 6 mV/V in the survey area, there are some anomalous zones with high chargeability over 10 mV/V. Apparent resistivities in this area ranged from 500 to 5000 ohm-m, with partially conductive zones less than 100 ohm-m and resistive zones over 5000 ohm-m.

Resistivity structures which synthetic resistivities were equivalent

roughly with observed apparent resistivity distribution on each survey lines was modeled, then high chargeability structures were modeled to give local high chargeability zones.

And then repeatedly model was modified to decrease differences between observed data and synthetic data up to minimize differences between observed data and synthetic data.

Two dimensional forward modeling results for each survey lines are given in Fig.2-4-12 through Fig.2-4-24.

As many high chargeability anomalies were located in high resistivity area, many high chargeability and high resistivity bodies were modeled. It was supposed that these high chargeability and high resistivity bodies consisted of hornblende-biotite granite, andesite and andesitic pyroclastic rocks with sulfide mineral dissemination.

Consequently only low resistivity body equal to or less than 433 ohm-m of sulfide ore in high chargeability body had possibility of being the target disseminated sulfide ore. On the other hand, there was possibility that high resistivity and high chargeability bodies were not sulfide, and contained a little disseminated sulfide.

The location and electrical properties of the anomalous bodies are given in the follows.

[Line A]

(1) A trapezoid anomaly of 28.6 mV/V , 865 ohm-m exits from No.11 to No.14 at the depth from 125 m to 530 m and dips to north-east.

(2) A triangle anomaly of 28.3 mV/V , 35 ohm-m exits from No.16 to No.18 at the depth from 100 m to 170 m.

[Line B]

(1) A trapezoid anomaly of 26.1 mV/V , 87 ohm-m exits from No.6 to No.8 at the depth from 50 m to 35 m.

(2) A six cornered polygonal anomaly of 50.1 mV/V , 305 ohm-m exits from No.12 to No.18 at the depth from 40 m to 360 m and dips to south-west.

[Line C]

(1) A rectangular anomaly of 50.0 mV/V , 400 ohm-m exits from No.7 to No.8 at the depth from 170 m to 450 m.

(2) A six cornered polygonal anomaly of 50.0 mV/V , 112 ohm-m exits from No.12 to No.19 at the depth from 140 m to 560 m.

[Line D]

(1) A trapezoid anomaly of 50.5 mV/V , 57 ohm-m exits from No.14 to No.16 at the depth from 120 m to 360 m.

[Line E]

(1) A polygonal anomaly of 55.5 mV/V , 257 ohm-m exits from No.9 to No.18 at the depth from 170 m to 580 m and dips to north-east.

[Line F]

(1) A trapezoid anomaly of 24.2 mV/V , 362 ohm-m exits from No.2 to No.5 at the depth from 160 m to 350 m.

(2) A trapezoid anomaly of 29.9 mV/V , 179 ohm-m exits from No.8 to No.12 at the depth from 110 m to 360 m and dips to south-west.

[Line G]

(1) A trapezoid anomaly of 36.7 mV/V , 878 ohm-m exits from No.3 to No.7 at the depth from 240 m to 550 m.

(2) A trapezoid anomaly of 20.0 mV/V , 750 ohm-m exits from No.14 to No.17 at the depth from 30 m to 270 m.

[Line H]

(1) A trapezoid anomaly of 20.0 mV/V , 263 ohm-m exits from No.6 to No.7 at the depth from 100 m to 220 m.

[Line I]

(1) A trapezoid anomaly of 17.6 mV/V , 125 ohm-m exits from No.1 to No.4 at the depth from 30 m to 190 m and dips to north-east.

[Line J]

(1) A reversed triangle anomaly of 22 mV/V , 593 ohm-m exits from No.1 to No.7 at the depth from 60 m to 340 m.

(2) A triangle anomaly of 53 mV/V , 129 ohm-m exits from No.10 to No.13 at the depth from 90 m to 310 m.

[Line K]

No low resistivity less than 1000 ohm-m and high chargeability over than 10 mV/V body was modeled.

[Line L]

(1) A trapezoid anomaly of 49.2 mV/V, 361 ohm-m exists from No.15 to No.18 at the depth from 240 m to 550 m.

4-4 Estimation of Geophysical Survey Anomalies

Comprehensive analysis of geophysical survey is shown in Fig.2-4-25.

Anomalous bodies of resistivity less than 1000 ohm-m and chargeability over than 10 mV/V modeled in geophysical survey were classified into four groups by its locality.

<a> Anomalous bodies located near La Guanaca mineralized zone

Line	Location	Resistivity ohm-m	Chargeability mV/V
A	No.11 to No.14	865	29.6
A	No.16 to No.18	35	28.3
B	No.12 to No.18	305	50.1
C	No.12 to No.18	113	50.0
D	No.14 to No.16	57	50.5
E	No. 8 to No.18	257	55.5

These anomalous bodies which extend from La Guanaca mineralized zone are located in the area underlain by Atacama conglomerate formation. They were analyzed and modeled in low resistivity and high chargeability area. But, as these bodies of low resistivity and high chargeability were analyzed from poor data near lower limit of detection. Therefore these should not show exact promising zones in this area.

 Anomalous bodies located near Rinconada de Villanueva mineralized zone

Line	Location	Resistivity ohm-m	Chargeability mV/V
F	No. 8 to No.12	444	30.0
G	No.14 to No.17	750	20.0

J	No.10 to No.13	129	53.1
L	No.15 to No.18	361	49.2

A anomalous body located from No.10 to No.13 on line J was modeled normally as a body of 129 ohm-m and 53.1 mV/V in low resistivity and high chargeability area. As being located near mineralized zone, this anomalous body is remarkable.

<c> Anomalous bodies located near central mineralized zone

Line	Location	Resistivity ohm-m	Chargeability mV/V
B	No. 6 to No. 8	87	26.1
C	No. 7 to No. 8	400	50.0

There is a possibility that these anomalous bodies should reflect the existence of sulfide ore, but also should reflect sulfide disseminated granodiorite or andesite with high resistivity.

<d> Anomalous bodies located south western part of the survey area

Line	Location	Resistivity ohm-m	Chargeability mV/V
G	No. 3 to No. 6	878	36.7
H	No. 6 to No. 7	263	20.0
I	No. 1 to No. 4	124	17.6
J	No. 1 to No. 7	593	22.0

They are located in high resistivity area and there is a possibility that these should reflect sulfide disseminated granodiorite with high resistivity.

As a result of geophysical survey, extracted promising areas are as follows.

- 1) Between No.10 and No.13 on line J
- 2) Between No.6 and No.8 on line B

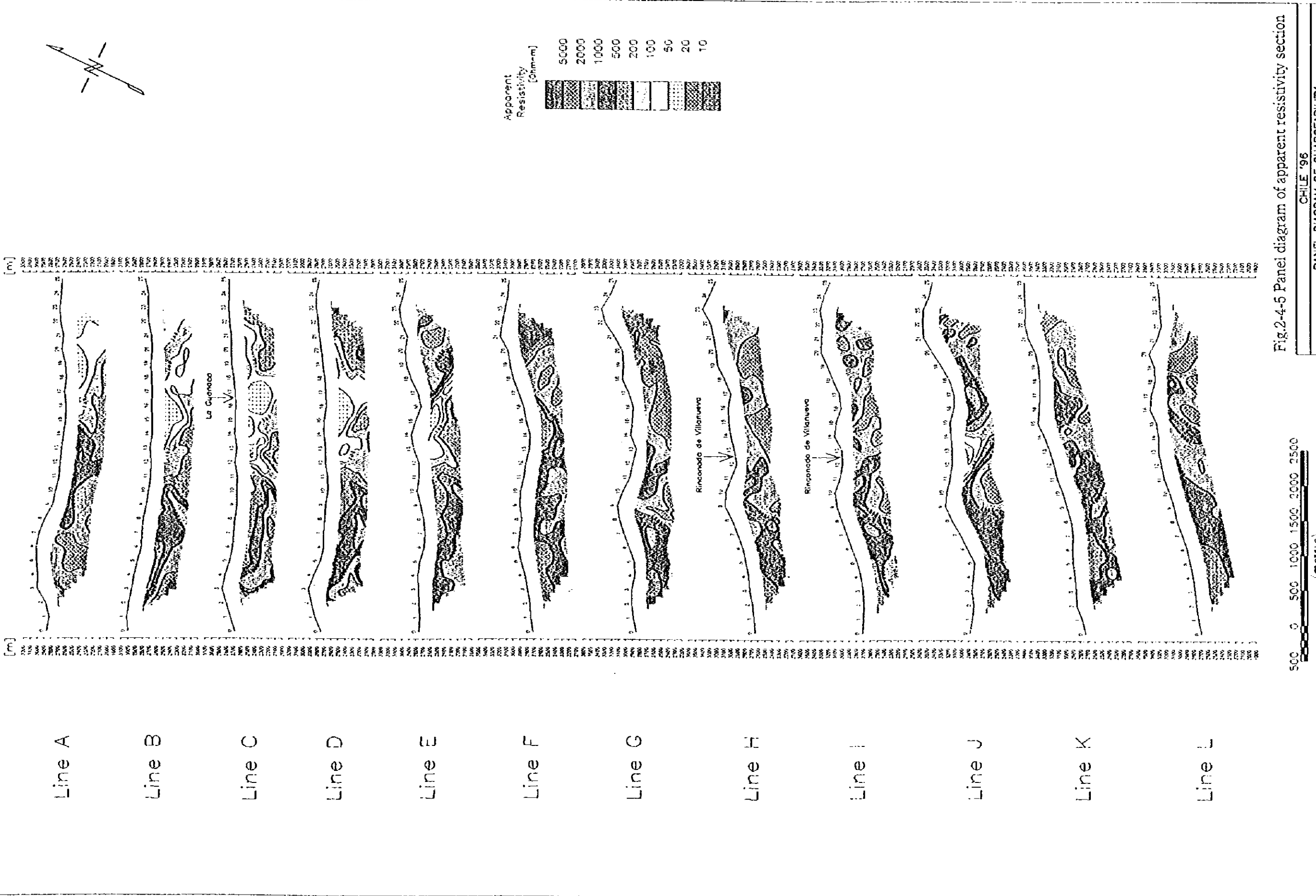


Fig.2-4-5 Panel diagram of apparent resistivity section

CHILE '96
PANEL DIAGRAM OF CHARGEABILITY

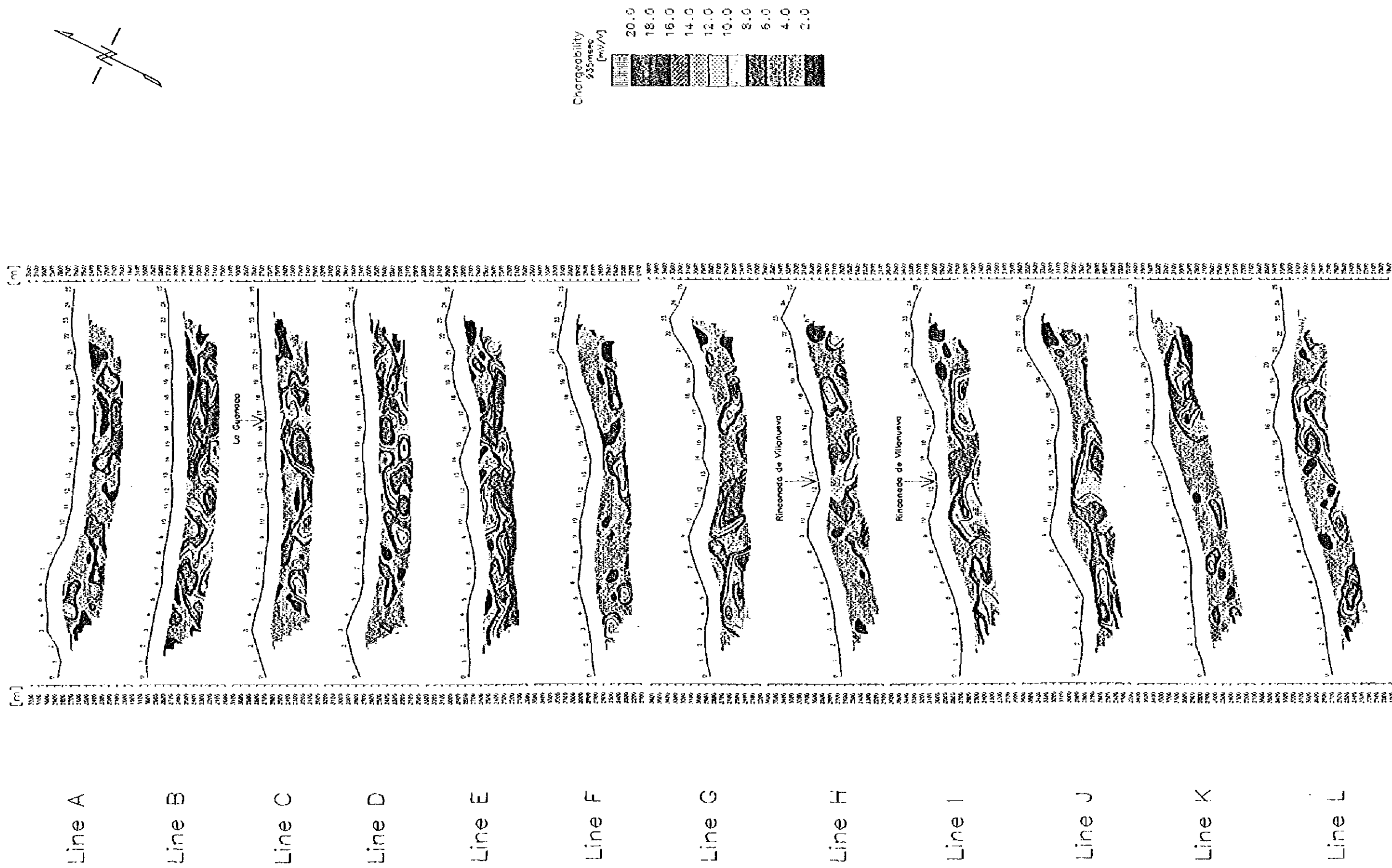


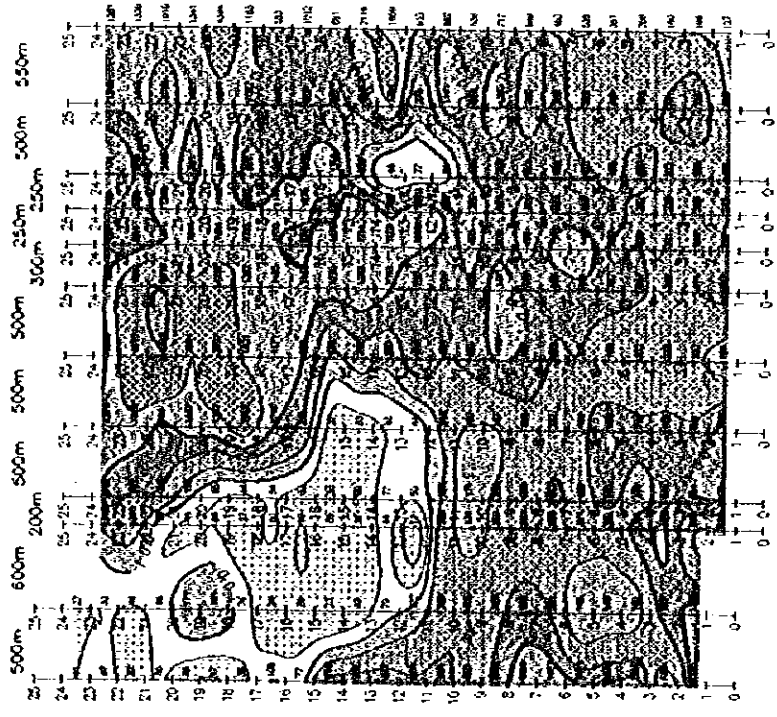
Fig.2-4-6 Panel diagram of chargeability section

500 0 500 1000 1500 2000 2500
(metres)

CHILE '96
PANEL DIAGRAM OF APPARENT RESISTIVITY

APPARENT RESISTIVITY PLAN

N=1



CHARGEABILITY PLAN

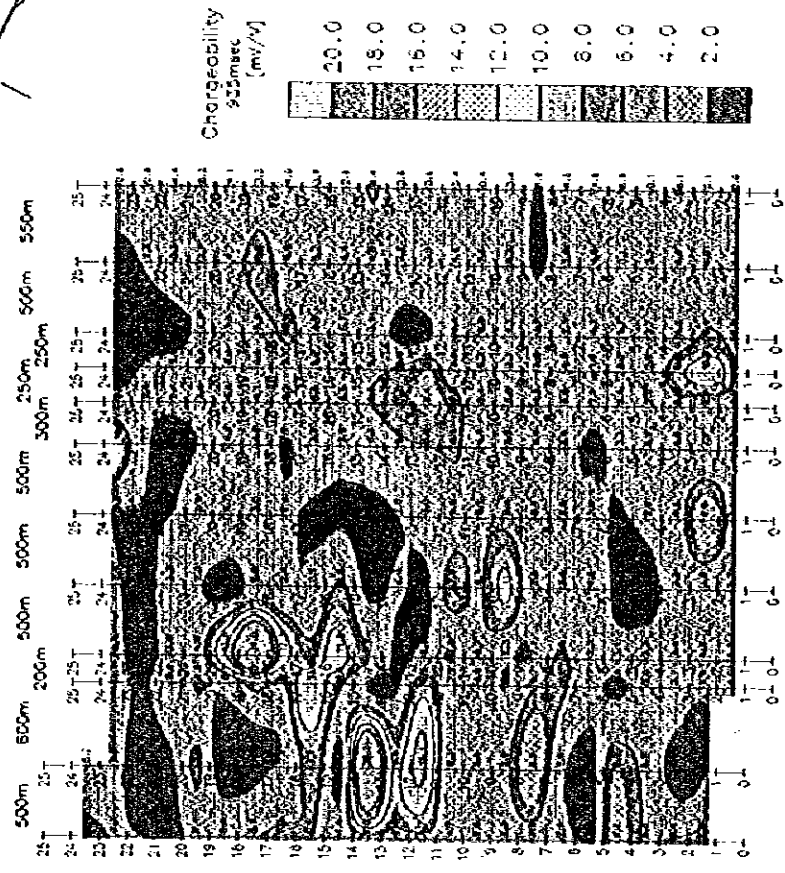
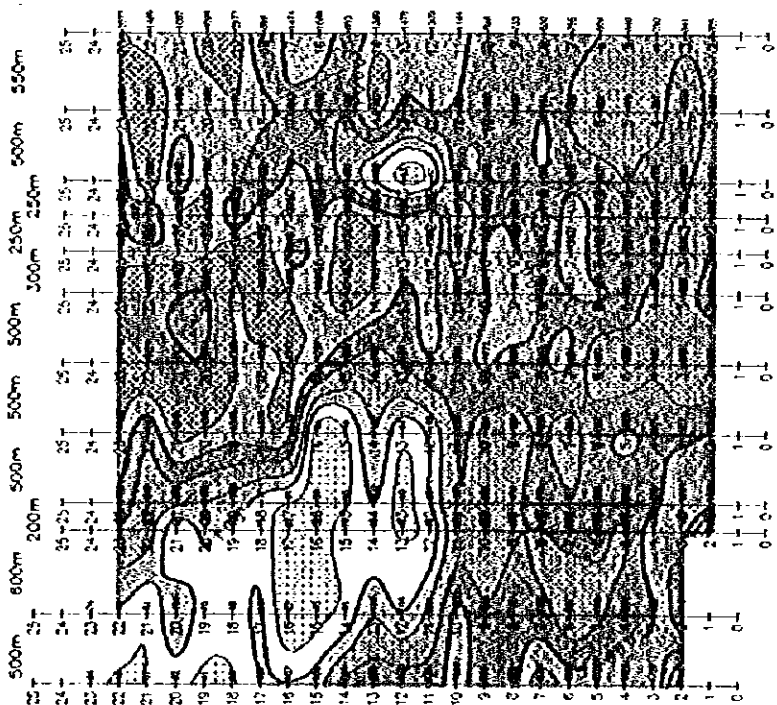


Fig.2-4-7 Plan of apparent resistivity and chargeability (n=1)

CHILE '96
PLAN
Apparent resistivity, Chargeability N=1
Time Domain IP Survey in Guanaca Area
(OCT 1996 - DEC 1996)
JAPAN-CHILE

APPARENT RESISTIVITY PLAN

N=2



CHARGEABILITY PLAN

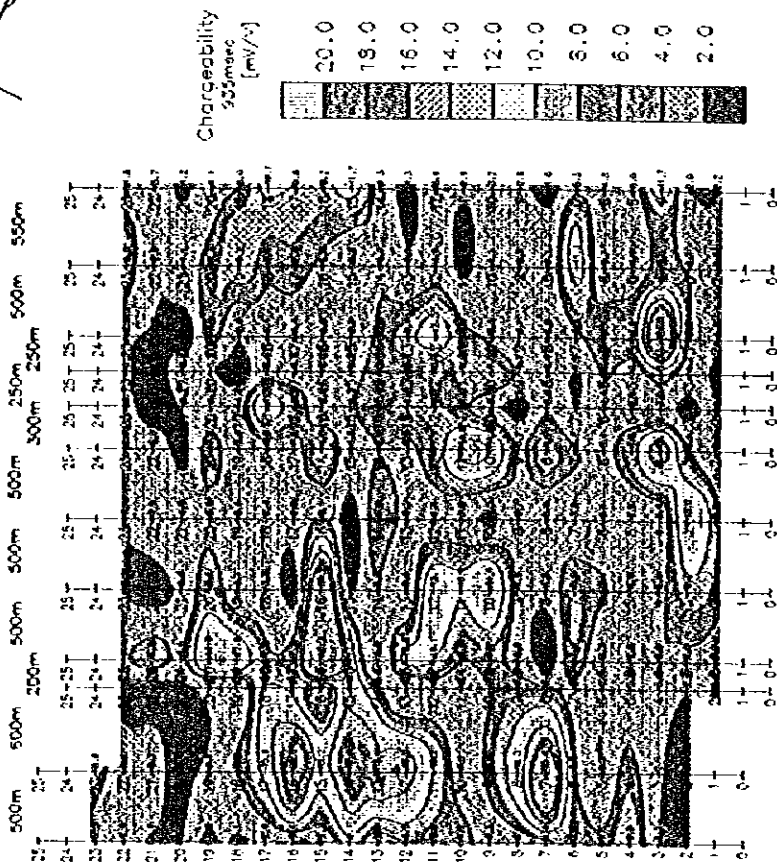
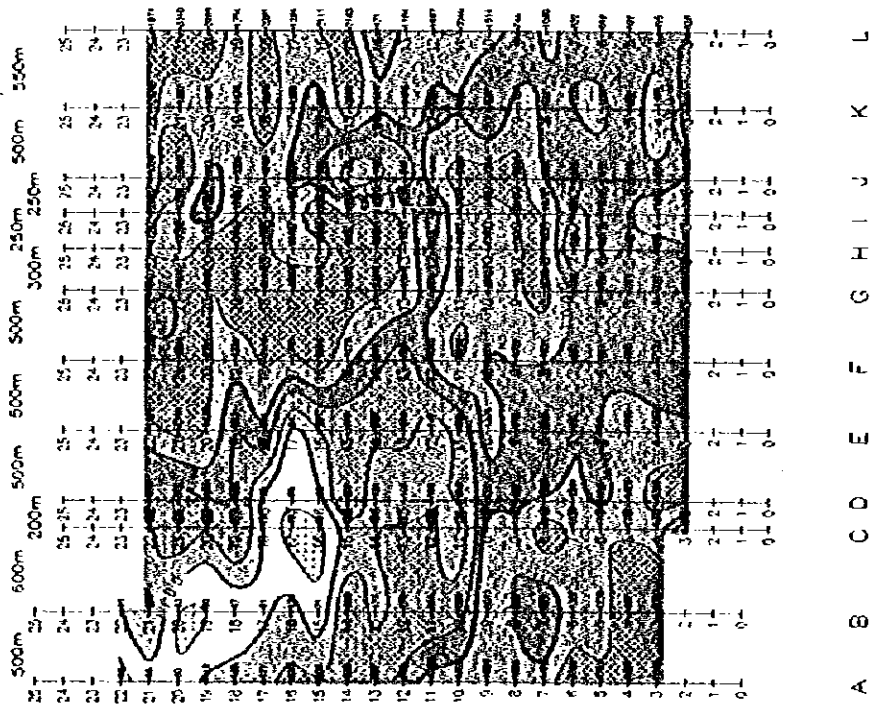


Fig.2-4-8 Plan of apparent resistivity and chargeability (n=2)

CHILE '96
PLAN
Apparent resistivity, Chargeability N=2
Time Domain IP Survey in Guanaca Area
(OCT 1996 - DEC 1996)
JAPAN-CHILE

N=4

APPARENT RESISTIVITY PLAN



CHARGEABILITY PLAN

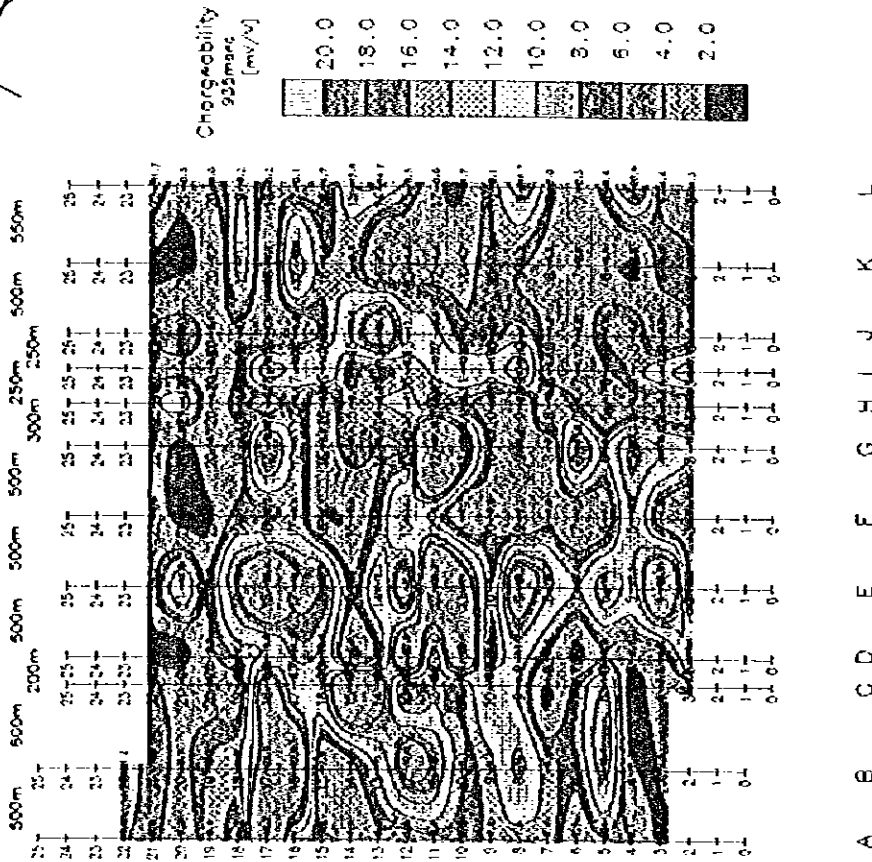
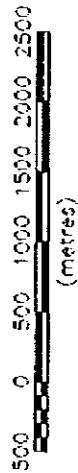


Fig.2-4-10 Plan of apparent resistivity and chargeability (n=4)



CHILE '96

PLAN

Apparent resistivity, Chargeability N=4

Time Domain IP Survey in Guanaca Area
(OCT 1996 - DEC 1996)

JAPAN-CHILE

